CMS Draft Analysis Note

The content of this note is intended for CMS internal use and distribution only

Background Combination Procedure for the searches for direct electroweak chargino and neutralino production with three or more leptons using 9.2 fb^{-1} of $\sqrt{s} = 8$ TeV CMS data

SUSY Multilepton EWKino Working Group
CERN

Abstract

We present the procedure used for the combination of background estimates in multi-lepton channels in the EWKino search. Because multiple groups are providing results in three and four lepton channels using a variety of different techniques, different methods are used to combine different types of backgrounds in each channel. The methods by which the background estimates are obtained are discussed elsewhere.

1 Introduction

The search for direct electroweak production of SUSY particles in multilepton modes [1] combines search regions with two or more leptons with different requirements on $E_{\mathrm{T}}^{\mathrm{miss}}$, M_{T}, dijet mass, lepton pair mass, and others to maximize sensitivity to different types of electroweak production. In the three and four lepton channels, multiple groups have designed and validated a variety of methods to estimate and understand the various contributions to background models. These methods are discussed elsewhere [2–5]. In this note, we restrict ourselves to discussing the procedure for the combination of these estimates in a way that maximizes consistency. We provide justification for assumptions and choices made to accomplish this goal.

2 Rare Processes

The background estimates for rare processes are taken from the simulation samples described in Table 1 by all three groups. Therefore, the estimates from these sources are synchronized and the resulting contributions are used.

Table 1: Summary of the MC samples for rare Standard Model processes. All datasets are produced with the MADGRAPH generator.

DBS Name	σ (pb)
/DYJetsToLL_M-50_TuneZ2Star_8TeV-madgraph-tarball/Summer12_DR53X-PU_S10_START53_V7A-v1	3532.8
/DYJetsToLL_M-10To50filter_8TeV-madgraph/Summer12_DR53X-PU_S10_START53_V7A-v1	—
/TTJets_MassiveBinDECAY_TuneZ2star_8TeV-madgraph-tauola/Summer12_DR53X-PU_S10_START53_V7A-v1	225.2
/TTZJets_8TeV-madgraph_v2/Summer12_DR53X-PU_S10_START53_V7A-v1	0.208
/TTWJets_8TeV-madgraph/Summer12_DR53X-PU_S10_START53_V7A-v1	0.232
/TTGJets_8TeV-madgraph/Summer12_DR53X-PU_S10_START53_V7A-v1	2.166
/ZZZNoGstarJets_8TeV-madgraph/Summer12_DR53X-PU_S10_START53_V7A-v1	0.01922
/WWWJets_8TeV-madgraph/Summer12_DR53X-PU_S10_START53_V7A-v1	0.08217
/ZZJetsTo4L_TuneZ2star_8TeV-madgraph-tauola/Summer12_DR53X-PU_S10_START53_V7A-v1	0.1769
/ZZJetsTo2L2Q_TuneZ2star_8TeV-madgraph-tauola/Summer12_DR53X-PU_S10_START53_V7A-v1	2.4487
/ZZJetsTo2L2Nu_TuneZ2star_8TeV-madgraph-tauola/Summer12_DR53X-PU_S10_START53_V7A-v3	0.3648
/WZJetsTo3LNu_TuneZ2_8TeV-madgraph-tauola/Summer12_DR53X-PU_S10_START53_V7A-v1	1.0575
/WZJetsTo2L2Q_TuneZ2star_8TeV-madgraph-tauola/Summer12_DR53X-PU_S10_START53_V7A-v1	2.206
/WWJetsTo2L2Nu_TuneZ2star_8TeV-madgraph-tauola/Summer12_DR53X-PU_S10_START53_V7A-v1	5.8123
/WJetsToLNu_TuneZ2Star_8TeV-madgraph-tarball/Summer12_DR53X-PU_S10_START53_V7A-v1	37509
/TTWWJets_8TeV-madgraph/Summer12_DR53X-PU_S10_START53_V7A-v1	0.002
/WWGJets_8TeV-madgraph/Summer12_DR53X-PU_S10_START53_V7A-v1	1.44
/WWZNoGstarJets_8TeV-madgraph/Summer12_DR53X-PU_S10_START53_V7A-v1	0.0633
/WZZNoGstarJets_8TeV-madgraph/Summer12_DR53X-PU_S10_START53_V7A-v1	0.01922

3 Internal Conversion and ZZ

The authors of [2] and [4] use separate data-driven methods to estimate the internal conversion background to light leptons and an official production of ZZJets to estimate the ZZ irreducible background. The authors of [3] use a private simulation sample that combines the ZZ irreducible background with the internal conversion background. We take the data-driven estimate described in [4, 5] and a synchronized estimate to account for the ZZ irreducible background.

4   WZ

WZ production makes up the largest irreducible background for three lepton search regions. The main source of the background estimation comes from the official WZ simulation sample. However, two of the groups apply corrections to make sure that the MET distribution is modeled properly [2, 4]. The data-driven corrections are found to be small and the final result is computed as a simple average of three predictions.

5   Fake leptons

The three groups have a variety of ways to estimate the backgrounds from fake leptons (both light leptons and taus). Because one group [2] includes the contribution from $t\bar{t}$ in their data-driven estimate, we average the data-driven contributions summed with the $t\bar{t}$ simulation contribution used by the two groups in the three lepton channels. Because only two groups [3, 4] are providing the four lepton channels, we synchronize the $t\bar{t}$ contribution for the four lepton channels and average the data-driven backgrounds.

6   Final Tables for Tri-lepton Analyses

A graphical comparison of the background estimations to be averaged is shown in detail in appendix A. Here, the summarized results are presented in five tables:

- Table 2 contains observed yields and background prediction for each search region in a tri-lepton channel with an opposite sign same flavor lepton pair present (3ℓ).
- Table 3 - for a channel without an opposite sign same flavor lepton pair (no OSSF).
- Table 4 - for a channel with a same sign di-lepton and a hadronically decaying tau (SSτ). This result is fully based on Ref. [2].
- Table 5 - for a channel with an opposite sign opposite flavor di-lepton and a hadronically decaying tau ($e^{\pm}\mu^{\mp}\tau$). This result is provided only in Ref. [3].
- Table 6 - for a channel with an opposite sign same flavor di-lepton and a hadronically decaying tau (OSSFτ). This result is based on Refs. [3] and [4].

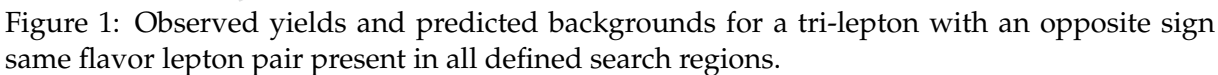The graphical representation of the combined results is shown in Figures 1, 2, 3, 4, 5.

Figure 1: Observed yields and predicted backgrounds for a tri-lepton with an opposite sign same flavor lepton pair present in all defined search regions.
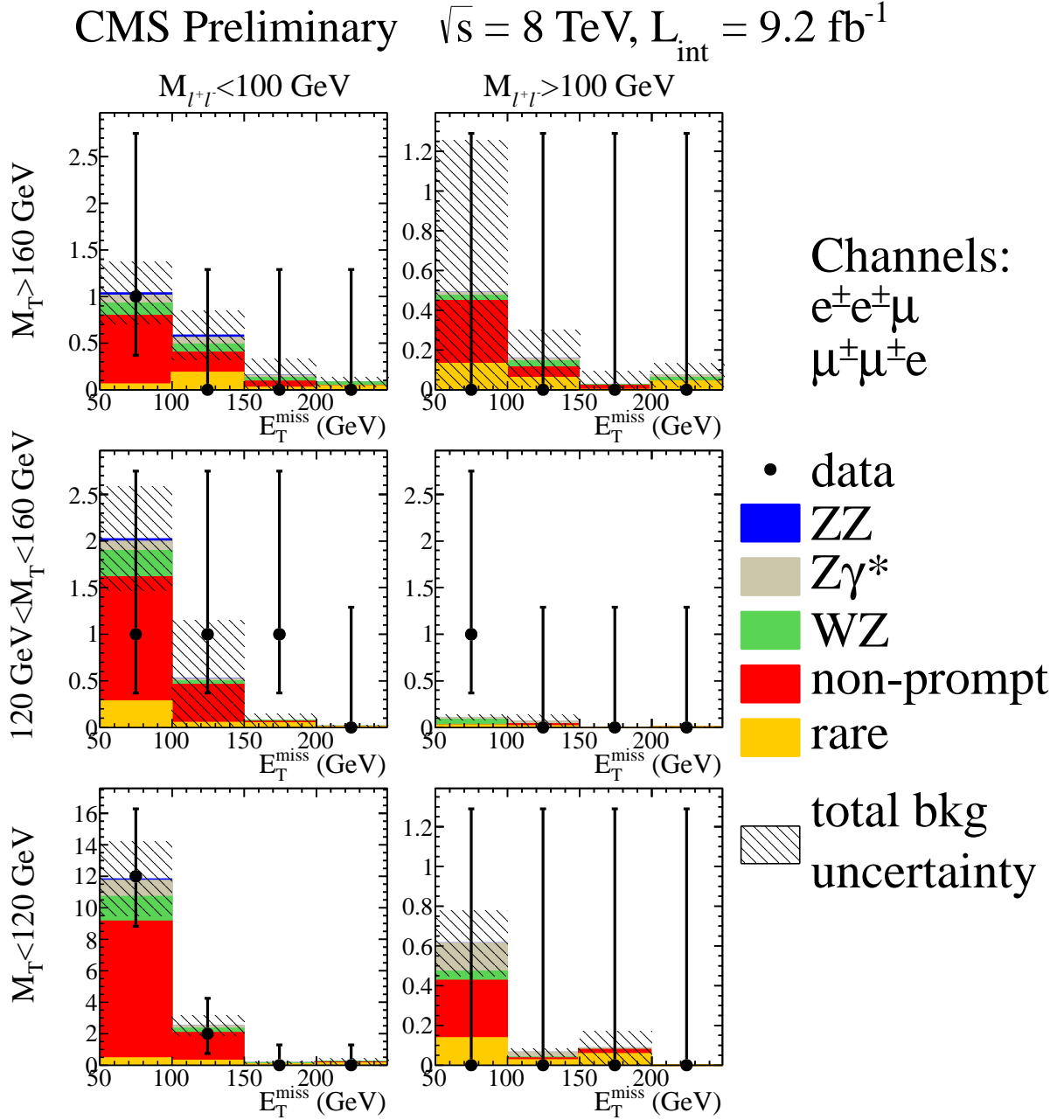
Figure 2: Observed yields and predicted backgrounds for a tri-lepton without an opposite sign same flavor lepton pair present in all defined search regions.
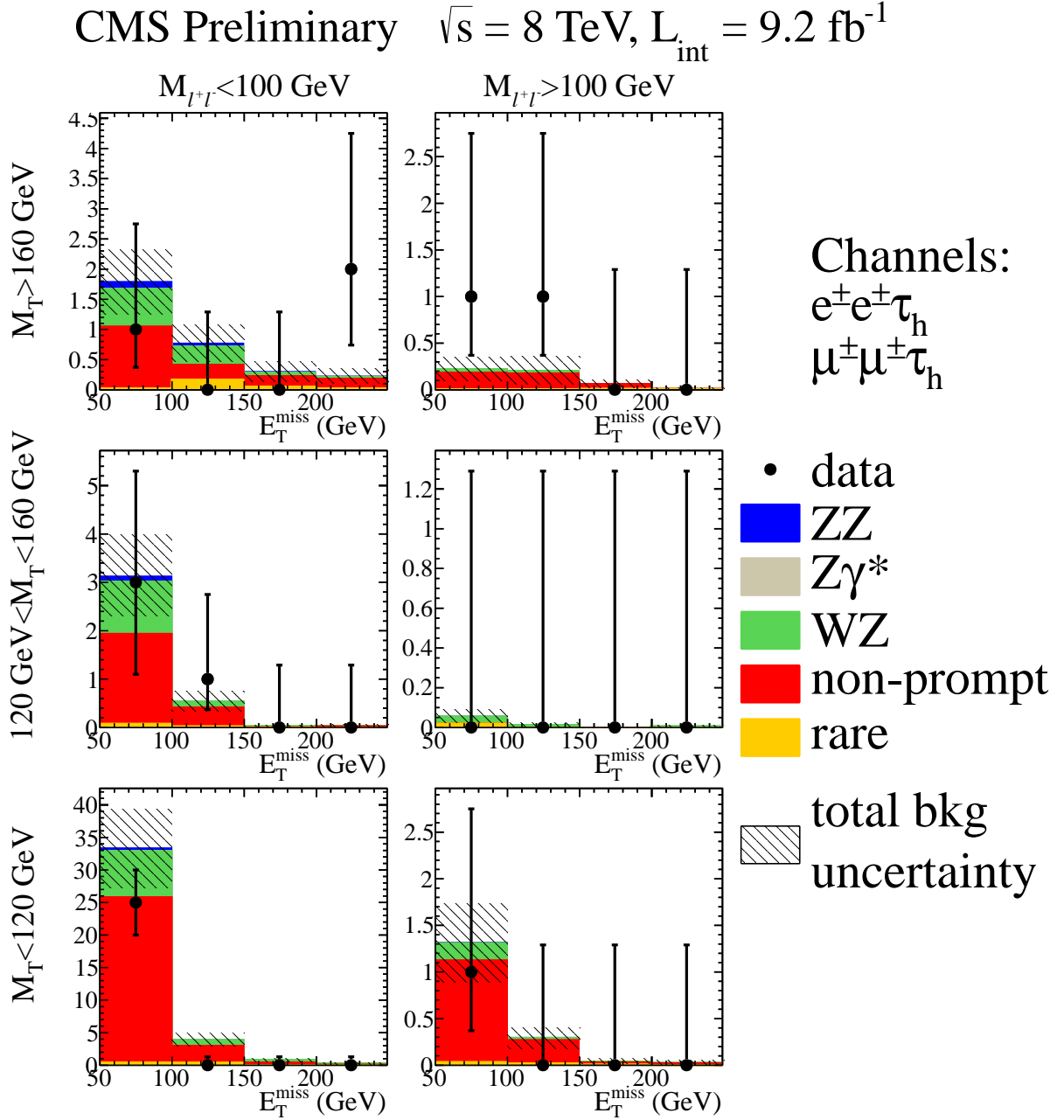
Figure 3: Observed yields and predicted backgrounds for a tri-lepton with a same sign di-lepton and a hadronically decaying tau in all defined search regions.
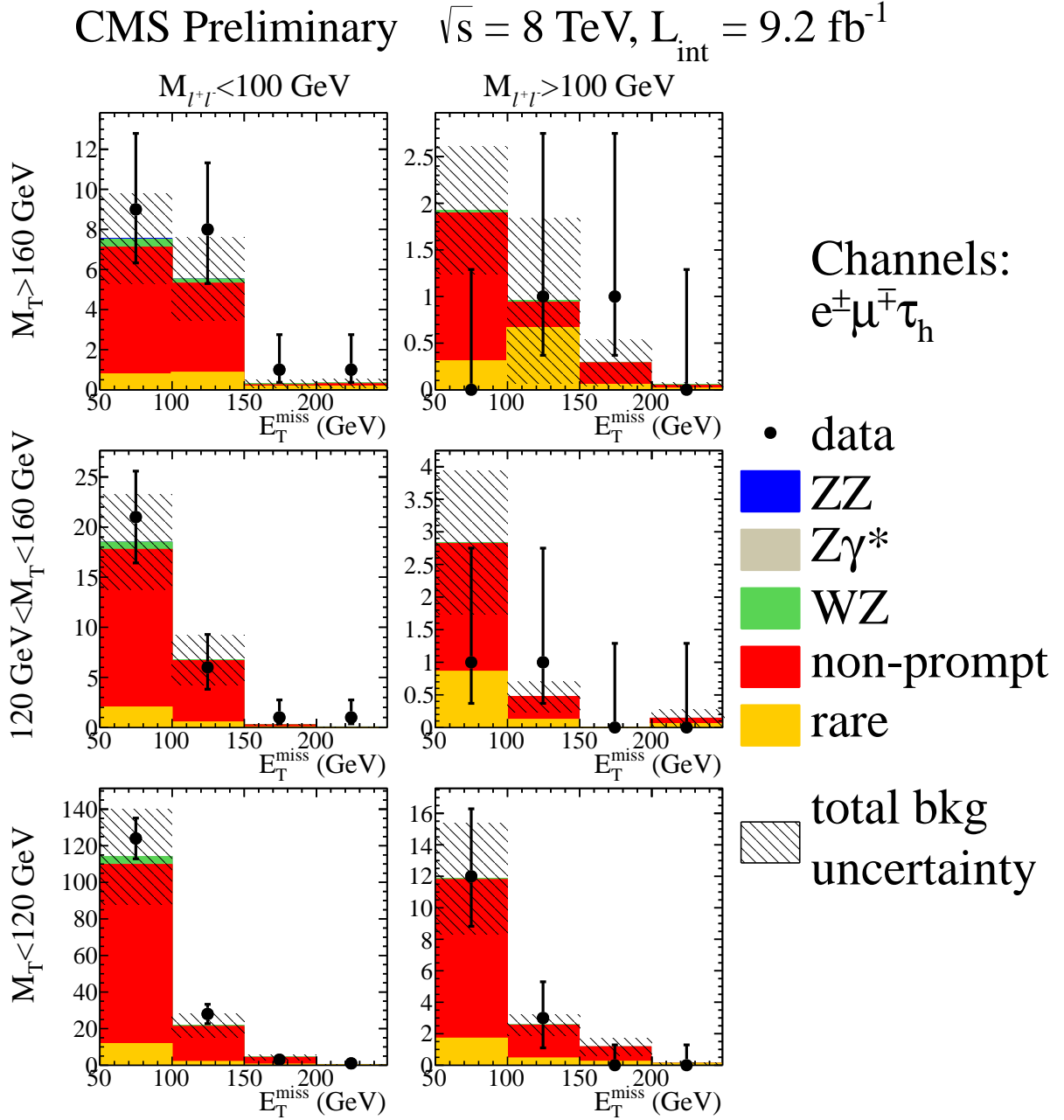
Figure 4: Observed yields and predicted backgrounds for a tri-lepton with an opposite sign opposite flavor di-lepton and a hadronically decaying tau in all defined search regions.
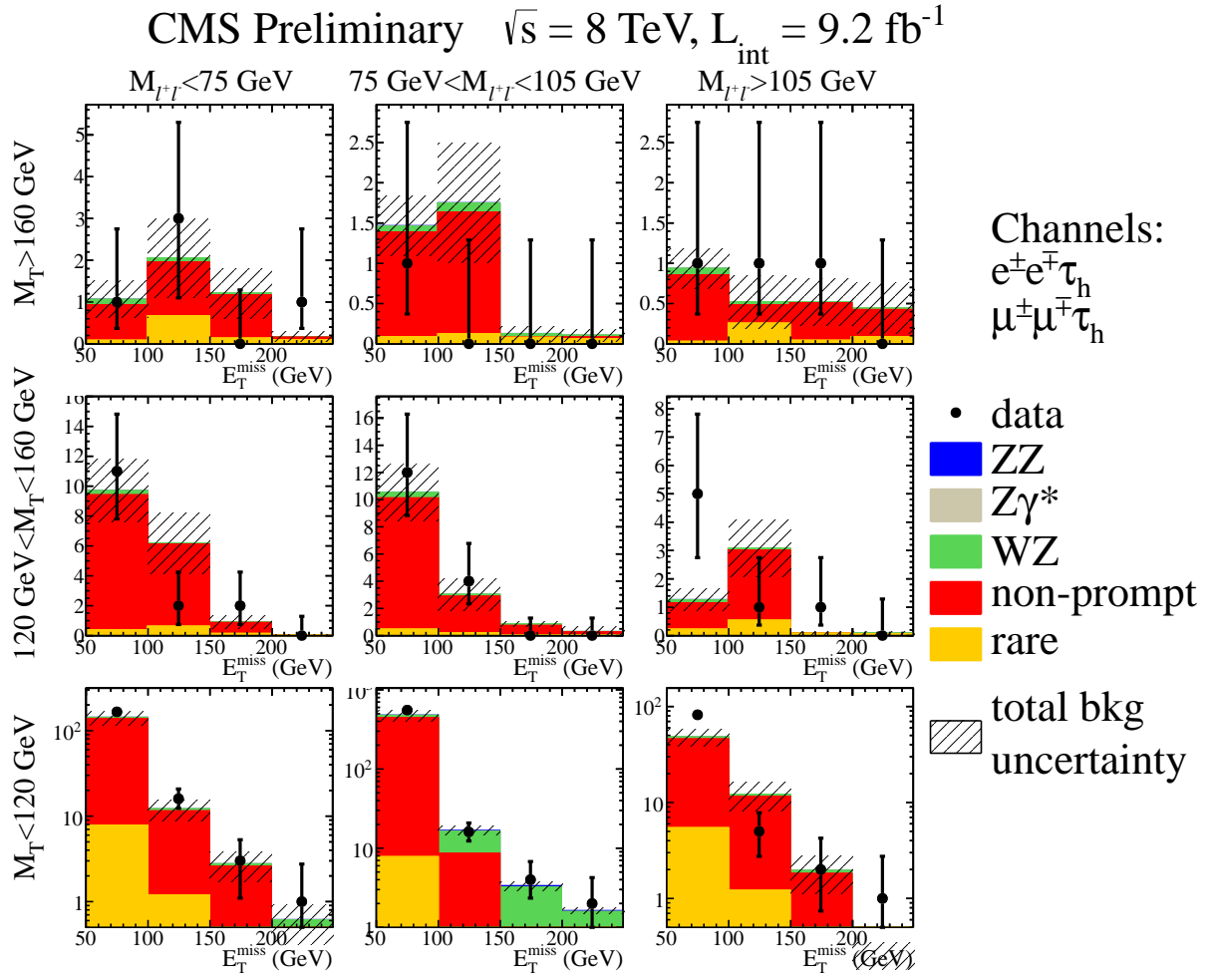
Figure 5: Observed yields and predicted backgrounds for a tri-lepton with an opposite sign same flavor di-lepton and a hadronically decaying tau in all defined search regions.

Table 2: The summary of the observed yields and predicted backgrounds for tri-lepton with opposite sign same flavor pair present.

E_T^{miss} (GeV)	WZ	Non-Prompt	Rare SM	$Z\gamma^*$	ZZ	Total bkg	Observed
$M_T > 160$ GeV, $M_{\ell\ell} < 75$ GeV							
50 – 100	0.76±0.077	0.98±0.42	0.16±0.19	0.13±0.017	0.081±0.011	2.1±0.46	4
100 – 150	0.59±0.067	0.9±0.38	0.096±0.11	0.023±0.003	0.045±0.0071	1.7±0.4	0
150 – 200	0.12±0.027	0.55±0.26	0.11±0.13	0±0	0.011±0.0028	0.79±0.3	1
> 200	0.13±0.029	0.073±0.19	0.033±0.038	0±0	0.0095±0.0025	0.25±0.2	0
$M_T > 160$ GeV, 75 GeV $< M_{\ell\ell} < 105$ GeV							
50 – 100	2.3±0.17	0.3±0.4	0.24±0.27	0.27±0.034	0.19±0.023	3.3±0.51	3
100 – 150	1.5±0.12	0.033±0.1	0.15±0.17	0.074±0.0095	0.064±0.0094	1.8±0.23	1
150 – 200	0.43±0.054	0.015±0.048	0.12±0.14	0.051±0.0065	0.015±0.0034	0.63±0.16	1
> 200	0.19±0.035	0.27±0.14	0.11±0.12	0±0	0.007±0.0021	0.58±0.19	1
$M_T > 160$ GeV, $M_{\ell\ell} > 105$ GeV							
50 – 100	0.46±0.058	0.11±0.02	0.5±0.66	0.13±0.016	0.025±0.0047	1.2±0.66	0
100 – 150	0.19±0.034	0.16±0.31	0.49±0.61	0.21±0.026	0.011±0.0028	1.1±0.69	1
150 – 200	0.083±0.022	0.033±0.068	0.14±0.17	0±0	0.0034±0.0014	0.26±0.18	0
> 200	0.042±0.016	0±0	0.11±0.14	0.025±0.0032	0.0036±0.0015	0.18±0.14	0
120 GeV $< M_T < 160$ GeV, $M_{\ell\ell} < 75$ GeV							
50 – 100	1.6±0.12	1.3±0.48	0.22±0.14	0.27±0.035	0.1±0.014	3.5±0.51	3
100 – 150	0.22±0.037	0.74±0.33	0.091±0.067	0.044±0.0056	0.015±0.0033	1.1±0.34	0
150 – 200	0.06±0.019	0.08±0.16	0.0046±0.0052	0±0	0.00099±0.00075	0.15±0.16	0
> 200	0.041±0.016	0±0	0.044±0.044	0.025±0.0032	0.00078±0.00067	0.11±0.047	0
120 GeV $< M_T < 160$ GeV, 75 GeV $< M_{\ell\ell} < 105$ GeV							
50 – 100	8.7±0.48	0.61±0.27	0.25±0.15	0.16±0.021	0.4±0.048	10±0.58	11
100 – 150	1.2±0.11	0.02±0.14	0.17±0.11	0±0	0.032±0.0056	1.5±0.21	0
150 – 200	0.16±0.031	0.17±0.41	0.071±0.054	0±0	0.0036±0.0015	0.4±0.42	1
> 200	0.13±0.028	0.029±0.092	0.014±0.014	0±0	0.0014±0.00089	0.17±0.097	1

$E_{\mathrm{T}}^{\mathrm{miss}}$ (GeV)	WZ	Non-Prompt	Rare SM	$Z\gamma^*$	ZZ	Total bkg	Observed
120 GeV $< M_{\mathrm{T}} <$ 160 GeV, $M_{\ell\ell} >$ 105 GeV							
$50-100$	0.57 ± 0.065	0.28 ± 0.16	0.11 ± 0.071	0.32 ± 0.041	0.039 ± 0.0064	1.3 ± 0.19	0
$100-150$	0.09 ± 0.023	0.00033 ± 0.00038	0.055 ± 0.047	0.025 ± 0.0032	0.0032 ± 0.0014	0.17 ± 0.053	2
$150-200$	0.027 ± 0.013	0.035 ± 0.092	0.054 ± 0.048	0 ± 0	0 ± 0	0.12 ± 0.1	0
>200	0.0018 ± 0.0043	0 ± 0	0.077 ± 0.086	0 ± 0	0 ± 0	0.079 ± 0.086	0
$M_{\mathrm{T}} <$ 120 GeV, $M_{\ell\ell} <$ 75 GeV							
$50-100$	25 ± 1.2	17 ± 4.1	1.4 ± 0.84	7.8 ± 1	1.3 ± 0.15	53 ± 4.5	63
$100-150$	3.1 ± 0.2	2.9 ± 0.95	0.42 ± 0.24	0.035 ± 0.0044	0.1 ± 0.014	6.6 ± 1	5
$150-200$	0.83 ± 0.081	0.36 ± 0.2	0.19 ± 0.13	0.015 ± 0.0019	0.018 ± 0.0038	1.4 ± 0.25	1
>200	0.35 ± 0.048	0.056 ± 0.15	0.082 ± 0.058	0.05 ± 0.0063	0.0083 ± 0.0024	0.54 ± 0.17	1
$M_{\mathrm{T}} <$ 120 GeV, 75 GeV $< M_{\ell\ell} <$ 105 GeV							
$50-100$	335 ± 14.6	20.8 ± 3.57	4.03 ± 2.18	9.49 ± 1.21	13.1 ± 1.49	382 ± 15.3	377
$100-150$	58 ± 2.8	2.3 ± 0.82	1.8 ± 1	0.071 ± 0.009	1.6 ± 0.19	63 ± 3.1	61
$150-200$	14 ± 0.76	0.38 ± 0.17	0.63 ± 0.35	0.0024 ± 0.00031	0.37 ± 0.044	16 ± 0.86	13
>200	8.7 ± 0.49	0.045 ± 0.085	0.55 ± 0.3	0.031 ± 0.0039	0.15 ± 0.02	9.5 ± 0.58	3
$M_{\mathrm{T}} <$ 120 GeV, $M_{\ell\ell} >$ 105 GeV							
$50-100$	12 ± 0.62	4.8 ± 1.4	1.2 ± 0.7	0.67 ± 0.086	0.6 ± 0.07	19 ± 1.7	22
$100-150$	2.3 ± 0.16	1 ± 0.44	0.53 ± 0.3	0.035 ± 0.0045	0.091 ± 0.012	4 ± 0.56	6
$150-200$	0.6 ± 0.067	0.11 ± 0.24	0.078 ± 0.047	0.05 ± 0.0064	0.029 ± 0.0052	0.87 ± 0.25	2
>200	0.36 ± 0.05	0.028 ± 0.054	0.029 ± 0.02	0 ± 0	0.014 ± 0.0031	0.43 ± 0.076	2

Table 3: The summary of the observed yields and predicted backgrounds for tri-lepton without opposite sign same flavor pair present.

E_T^{miss} (GeV)	WZ	Non-Prompt	Rare SM	$Z\gamma^*$	ZZ	Total bkg	Observed
$M_T > 160$ GeV, $M_{\ell\ell} < 100$ GeV							
50 − 100	0.13±0.028	0.74±0.32	0.058±0.068	0.085±0.01	0.026±0.0048	1±0.33	1
100 − 150	0.089±0.023	0.22±0.14	0.18±0.23	0.069±0.0085	0.028±0.0051	0.59±0.27	0
150 − 200	0.038±0.015	0.066±0.17	0.022±0.026	0.026±0.0031	0.0037±0.0015	0.16±0.17	0
> 200	0.038±0.015	0.0014±0.00081	0.039±0.047	0±0	0.0043±0.0016	0.083±0.049	0
$M_T > 160$ GeV, $M_{\ell\ell} > 100$ GeV							
50 − 100	0.025±0.012	0.32±0.75	0.13±0.16	0.016±0.0021	0.0012±0.00083	0.49±0.76	0
100 − 150	0.03±0.013	0.053±0.12	0.06±0.076	0.012±0.0016	0.0026±0.0012	0.16±0.14	0
150 − 200	0.0034±0.0067	0.021±0.067	0.00061±0.00073	0±0	0.0014±0.00089	0.027±0.067	0
> 200	0.017±0.0097	0±0	0.044±0.058	0.013±0.0016	0±0	0.073±0.059	0
120 GeV $< M_T < 160$ GeV, $M_{\ell\ell} < 100$ GeV							
50 − 100	0.28±0.041	1.3±0.51	0.28±0.22	0.098±0.013	0.029±0.0053	2±0.56	1
100 − 150	0.041±0.015	0.41±0.63	0.051±0.036	0.019±0.0025	0.0042±0.0016	0.52±0.63	1
150 − 200	0.015±0.0093	0.015±0.047	0.047±0.046	0±0	0±0	0.077±0.066	1
> 200	0.003±0.0039	0.003±0.0017	0.0068±0.0062	0.013±0.0016	0±0	0.013±0.0075	0
120 GeV $< M_T < 160$ GeV, $M_{\ell\ell} > 100$ GeV							
50 − 100	0.059±0.018	0±0	0.023±0.019	0.022±0.0029	0.00088±0.00071	0.11±0.026	1
100 − 150	0.0037±0.0083	0.021±0.067	0.014±0.014	0.025±0.0032	0±0	0.064±0.069	0
150 − 200	0±0	0±0	0.00021±0.00019	0±0	0±0	0.00021±0.00019	0
> 200	0±0	0±0	0.004±0.0046	0±0	0±0	0.004±0.0046	0
$M_T < 120$ GeV, $M_{\ell\ell} < 100$ GeV							
50 − 100	1.6±0.12	8.7±2.3	0.44±0.26	1±0.13	0.11±0.015	12±2.4	12
100 − 150	0.27±0.042	1.8±0.6	0.29±0.18	0.18±0.023	0.01±0.0026	2.5±0.63	2
150 − 200	0.079±0.022	1.7e-06±2e-06	0.062±0.05	0.012±0.0019	0.0023±0.0012	0.16±0.055	0
> 200	0.031±0.013	0.058±0.17	0.13±0.14	0.016±0.002	0.00099±0.00075	0.24±0.22	0
$M_T < 120$ GeV, $M_{\ell\ell} > 100$ GeV							
50 − 100	0.047±0.017	0.29±0.14	0.14±0.086	0.14±0.018	0.0021±0.0011	0.61±0.16	0
100 − 150	0.0043±0.005	0.0092±0.0053	0.025±0.019	0.026±0.0033	0±0	0.065±0.02	0
150 − 200	0±0	0.021±0.067	0.056±0.049	0.0083±0.0011	0.00011±0.00025	0.086±0.083	0
> 200	0±0	0±0	0.00021±0.00017	0±0	0±0	0.00021±0.00017	0

Table 4: The summary of the observed yields and predicted backgrounds for the channel with a same sign di-lepton and a hadronically decaying tau.

E_T^{miss} (GeV)	WZ	Non-Prompt	Rare SM	$Z\gamma^*$	ZZ	Total bkg	Observed
50 – 100	0.62±0.32	1±0.37	0.029±0.019	0±0	0.12±0.06	1.8±0.54	1
100 – 150	0.3±0.15	0.25±0.14	0.17±0.11	0±0	0.05±0.025	0.77±0.31	0
150 – 200	0.061±0.035	0.17±0.15	0.056±0.036	0±0	0.013±0.0071	0.3±0.17	0
> 200	0.029±0.019	0.16±0.12	0.028±0.019	0±0	0.0065±0.0036	0.22±0.12	2
$M_T > 160$ GeV, $M_{\ell\ell} > 100$ GeV							
50 – 100	0.034±0.021	0.18±0.12	0.009±0.0069	0±0	0.0021±0.0014	0.22±0.13	1
100 – 150	0.025±0.017	0.17±0.15	0.0093±0.0069	0±0	0.0024±0.0015	0.21±0.15	1
150 – 200	0±0	0.053±0.041	0.012±0.012	0±0	0.00048±0.00049	0.065±0.043	0
> 200	0±0	0±0	0.011±0.0085	0±0	0.00027±0.00035	0.012±0.0086	0
120 GeV $< M_T < 160$ GeV, $M_{\ell\ell} < 100$ GeV							
50 – 100	1.1±0.55	1.9±0.55	0.08±0.046	0±0	0.11±0.054	3.1±0.84	3
100 – 150	0.12±0.062	0.39±0.19	0.027±0.018	0±0	0.0092±0.005	0.54±0.21	1
150 – 200	0.02±0.014	0±0	0.0095±0.01	0±0	0.0015±0.0011	0.031±0.02	0
> 200	0.0054±0.0058	0.022±0.023	0.0035±0.0034	0±0	0.00048±0.00049	0.032±0.024	0
120 GeV $< M_T < 160$ GeV, $M_{\ell\ell} > 100$ GeV							
50 – 100	0.035±0.022	0±0	0.02±0.015	0±0	0.0014±0.001	0.056±0.033	0
100 – 150	0.013±0.01	0±0	0.00015±0.00013	0±0	0±0	0.013±0.01	0
150 – 200	0±0	0±0	0±0	0±0	0±0	0±0	0
> 200	0.0065±0.0064	0±0	0±0	0±0	0±0	0.0065±0.0064	0
$M_T < 120$ GeV, $M_{\ell\ell} < 100$ GeV							
50 – 100	7.1±3.5	25±4.6	0.43±0.22	0±0	0.46±0.23	33±6.1	25
100 – 150	0.87±0.43	2.6±0.68	0.41±0.36	0±0	0.04±0.02	3.9±1	0
150 – 200	0.4±0.2	0.39±0.19	0.032±0.021	0±0	0.0063±0.0036	0.82±0.29	0
> 200	0.21±0.11	0.071±0.056	0.024±0.015	0±0	0.0033±0.002	0.31±0.14	0
$M_T < 120$ GeV, $M_{\ell\ell} > 100$ GeV							
50 – 100	0.18±0.097	1.1±0.41	0.035±0.023	0±0	0.0072±0.0039	1.3±0.42	1
100 – 150	0.025±0.017	0.25±0.11	0.02±0.014	0±0	0.0017±0.0012	0.29±0.11	0
150 – 200	0.011±0.0091	0.022±0.023	0.0083±0.0065	0±0	0.0005±0.00051	0.042±0.027	0
> 200	0.0047±0.0053	0.022±0.023	0.00011±0.00011	0±0	0±0	0.027±0.024	0

Table 5: The summary of the observed yields and predicted backgrounds for the channel with an opposite sign opposite flavor di-lepton and a hadronically decaying tau.

E_T^{miss} (GeV)	WZ	Non-Prompt	Rare SM	$Z\gamma^*$	ZZ	Total bkg	Observed
$50 - 100$	0.41±0.053	6.3±2.1	0.78±0.89	0±0	0.043±0.0069	7.5±2.2	9
$100 - 150$	0.21±0.036	4.4±1.8	0.85±0.97	0±0	0.026±0.0048	5.5±2.1	8
$150 - 200$	0.061±0.019	0.054±0.062	0.17±0.21	0±0	0.0071±0.0022	0.3±0.22	1
> 200	0.045±0.016	0.1±0.026	0.17±0.21	0±0	0.0059±0.0019	0.33±0.21	1
$M_T > 160$ GeV, $M_{\ell\ell} > 100$ GeV							
$50 - 100$	0.027±0.013	1.6±0.58	0.31±0.36	0±0	0.0012±0.00082	1.9±0.68	0
$100 - 150$	0.016±0.0095	0.27±0.15	0.66±0.87	0±0	0.00028±0.00039	0.95±0.89	1
$150 - 200$	0.007±0.0064	0.23±0.24	0.055±0.072	0±0	0±0	0.29±0.25	1
> 200	0.0088±0.0071	0.032±0.016	0.013±0.016	0±0	0.00079±0.00067	0.055±0.024	0
120 GeV $< M_T < 160$ GeV, $M_{\ell\ell} < 100$ GeV							
$50 - 100$	0.71±0.073	16±4.6	2±1.3	0±0	0.06±0.0089	19±4.8	21
$100 - 150$	0.076±0.021	6.1±2.5	0.51±0.33	0±0	0.0061±0.002	6.7±2.5	6
$150 - 200$	0.022±0.011	0.18±0.044	0.035±0.029	0±0	0.0017±0.00098	0.24±0.054	1
> 200	0.017±0.01	0±0	0.0072±0.0066	0±0	0.00098±0.00075	0.025±0.012	1
120 GeV $< M_T < 160$ GeV, $M_{\ell\ell} > 100$ GeV							
$50 - 100$	0.02±0.011	2±0.92	0.85±0.61	0±0	0.00086±0.0007	2.8±1.1	1
$100 - 150$	0±0	0.35±0.22	0.12±0.091	0±0	0±0	0.47±0.24	1
$150 - 200$	0±0	0±0	6.6e-05±7.5e-05	0±0	0±0	6.6e-05±7.5e-05	0
> 200	0±0	0.084±0.12	0.054±0.056	0±0	0±0	0.14±0.14	0
$M_T < 120$ GeV, $M_{\ell\ell} < 100$ GeV							
$50 - 100$	4.28±0.268	97.8±25.4	11.7±6.37	0±0	0.232±0.0286	114±26.2	124
$100 - 150$	0.65±0.07	19±6.4	1.8±1	0±0	0.026±0.0049	22±6.5	28
$150 - 200$	0.16±0.032	3.7±1.5	0.37±0.26	0±0	0.006±0.0019	4.3±1.5	3
> 200	0.12±0.026	0±0	0.14±0.098	0±0	0.0022±0.0011	0.25±0.1	1
$M_T < 120$ GeV, $M_{\ell\ell} > 100$ GeV							
$50 - 100$	0.083±0.022	10±3.4	1.7±0.96	0±0	0.0096±0.0026	12±3.5	12
$100 - 150$	0.028±0.013	2.1±0.63	0.43±0.26	0±0	0.00073±0.00064	2.5±0.68	3
$150 - 200$	2.4e-05±3.4e-05	0.93±0.53	0.22±0.15	0±0	0±0	1.1±0.55	0
> 200	0±0	0±0	0.095±0.073	0±0	0±0	0.095±0.073	0

Table 6: The summary of the observed yields and predicted backgrounds for the channel with an OSSF di-lepton and a hadronically decaying tau.

$E_\mathrm{T}^\mathrm{miss}$ (GeV)	WZ	Non-Prompt	Rare SM	$Z\gamma^*$	ZZ	Total bkg	Observed
$M_\mathrm{T} > 160$ GeV, $M_{\ell\ell} < 75$ GeV							
50 – 100	0.13±0.028	0.85±0.42	0.081±0.1	0±0	0.0096±0.0026	1.1±0.44	1
100 – 150	0.097±0.024	1.3±0.46	0.67±0.81	0±0	0.0049±0.0017	2.1±0.93	3
150 – 200	0.04±0.015	1±0.57	0.13±0.16	0±0	0.0016±0.00097	1.2±0.59	0
> 200	0.016±0.0095	0.061±0.031	0.091±0.11	0±0	0±0	0.17±0.12	1
$M_\mathrm{T} > 160$ GeV, 75 GeV $< M_{\ell\ell} < 105$ GeV							
50 – 100	0.067±0.02	1.3±0.36	0.087±0.1	0±0	0.012±0.0029	1.5±0.37	1
100 – 150	0.11±0.026	1.5±0.73	0.12±0.15	0±0	0.0073±0.0022	1.7±0.74	0
150 – 200	0.036±0.015	0.0088±0.0044	0.078±0.094	0±0	0.0023±0.0012	0.13±0.095	0
> 200	0.022±0.011	0.024±0.012	0.059±0.068	0±0	0±0	0.1±0.07	0
$M_\mathrm{T} > 160$ GeV, $M_{\ell\ell} > 105$ GeV							
50 – 100	0.079±0.022	0.83±0.25	0.029±0.043	0±0	0.0018±0.001	0.93±0.25	1
100 – 150	0.039±0.015	0.23±0.14	0.25±0.3	0±0	0.0021±0.0011	0.52±0.33	1
150 – 200	0.0071±0.0064	0.47±0.28	0.042±0.059	0±0	0.00058±0.00057	0.52±0.29	1
> 200	0.017±0.01	0.34±0.29	0.087±0.11	0±0	0.0012±0.00082	0.44±0.31	0
120 GeV $< M_\mathrm{T} < 160$ GeV, $M_{\ell\ell} < 75$ GeV							
50 – 100	0.27±0.042	9±2.1	0.38±0.25	0±0	0.033±0.0057	9.7±2.1	11
100 – 150	0.061±0.019	5.5±2	0.61±0.47	0±0	0.0031±0.0014	6.2±2	2
150 – 200	0.036±0.014	0.73±0.42	0.13±0.1	0±0	0±0	0.89±0.43	2
> 200	0.0099±0.0075	0.015±0.0074	0.019±0.021	0±0	0±0	0.044±0.024	0
120 GeV $< M_\mathrm{T} < 160$ GeV, 75 GeV $< M_{\ell\ell} < 105$ GeV							
50 – 100	0.39±0.052	9.7±2.1	0.45±0.29	0±0	0.043±0.0068	11±2.1	12
100 – 150	0.14±0.029	2.7±1.2	0.18±0.12	0±0	0.008±0.0023	3±1.2	4
150 – 200	0.1±0.025	0.69±0.17	0.04±0.026	0±0	0.0042±0.0016	0.83±0.18	0
> 200	0.032±0.014	0.2±0.35	0.044±0.036	0±0	0.00088±0.00071	0.28±0.35	0
120 GeV $< M_\mathrm{T} < 160$ GeV, $M_{\ell\ell} > 105$ GeV							
50 – 100	0.11±0.025	0.93±0.35	0.22±0.15	0±0	0.0053±0.0018	1.3±0.38	5
100 – 150	0.062±0.019	2.5±0.95	0.54±0.35	0±0	0.0026±0.0012	3.1±1	1
150 – 200	0.014±0.0089	0±0	0.073±0.061	0±0	0±0	0.087±0.062	1
> 200	0.018±0.01	0.01±0.0051	0.052±0.06	0±0	0±0	0.08±0.061	0
$M_\mathrm{T} < 120$ GeV, $M_{\ell\ell} < 75$ GeV							
50 – 100	4.16±0.262	131±25.7	7.78±4.3	0±0	0.533±0.0627	143±26.1	166
100 – 150	0.64±0.069	10±3.2	1.2±0.67	0±0	0.047±0.0073	12±3.3	16
150 – 200	0.18±0.033	2.5±1	0.064±0.049	0±0	0.0054±0.0018	2.8±1	3
> 200	0.11±0.026	0.47±0.3	0.028±0.024	0±0	0.0036±0.0015	0.61±0.3	1
$M_\mathrm{T} < 120$ GeV, 75 GeV $< M_{\ell\ell} < 105$ GeV							
50 – 100	32.6±1.71	433±80.6	7.76±4.23	0±0	5.05±0.574	478±80.7	554
100 – 150	7.6±0.44	7.7±2.1	0.85±0.48	0±0	0.62±0.072	17±2.2	16
150 – 200	2.5±0.17	0.57±0.36	0.17±0.099	0±0	0.13±0.017	3.3±0.41	4
> 200	1.4±0.11	0.083±0.042	0.092±0.054	0±0	0.056±0.0084	1.6±0.13	2
$M_\mathrm{T} < 120$ GeV, $M_{\ell\ell} > 105$ GeV							
50 – 100	2.2±0.16	40±9.5	5.4±3	0±0	0.36±0.043	48±10	82
100 – 150	0.48±0.058	10±3.9	1.2±0.81	0±0	0.058±0.0087	12±4	5
150 – 200	0.13±0.028	1.7±0.82	0.11±0.082	0±0	0.013±0.003	2±0.83	2
> 200	0.063±0.019	0.14±0.068	0.059±0.042	0±0	0.0061±0.002	0.26±0.082	1

7   Final Tables for Four Lepton Analyses

The summarized results are presented in three tables:

- Table 7 contains observed yields and background prediction for each search region in the four lepton channels

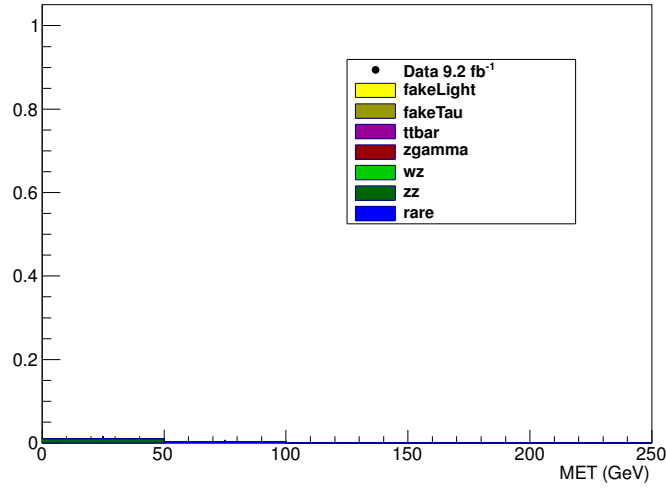The graphical representation of the results is shown in Figures 6, 7, 8, 10, 9, 11, 12, and 13.

Figure 6: Observed yields and predicted backgrounds for four lepton events with no OSSF pairs and zero taus.
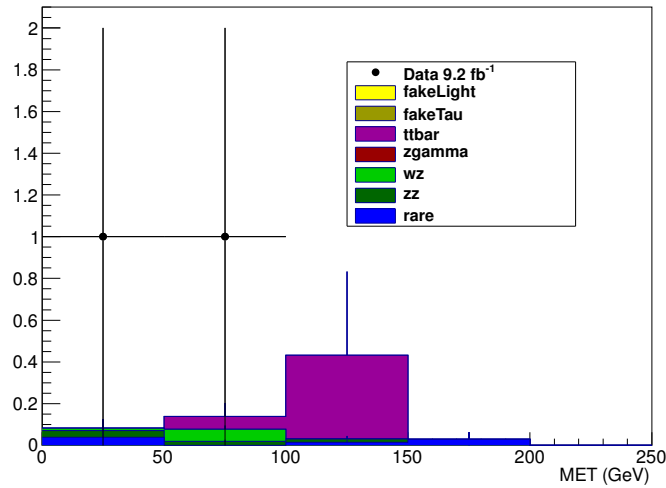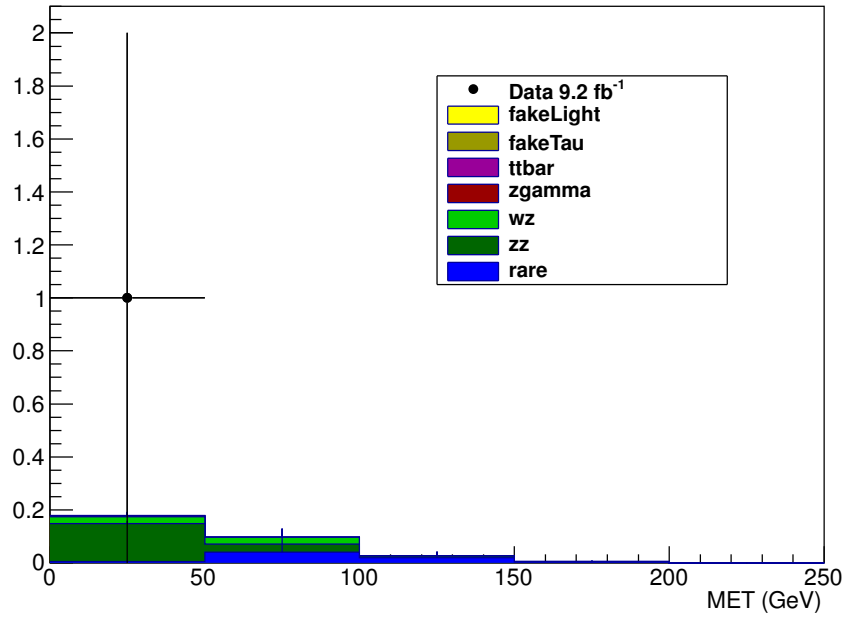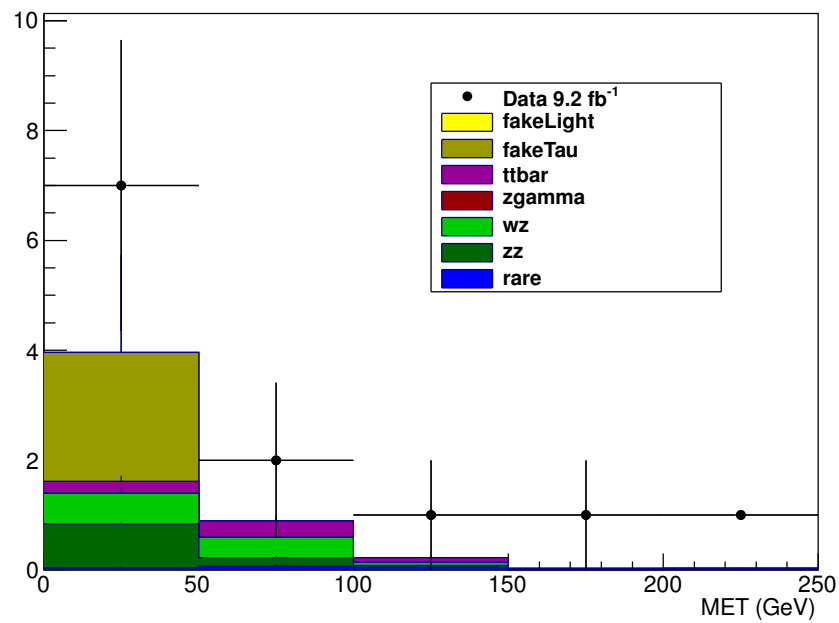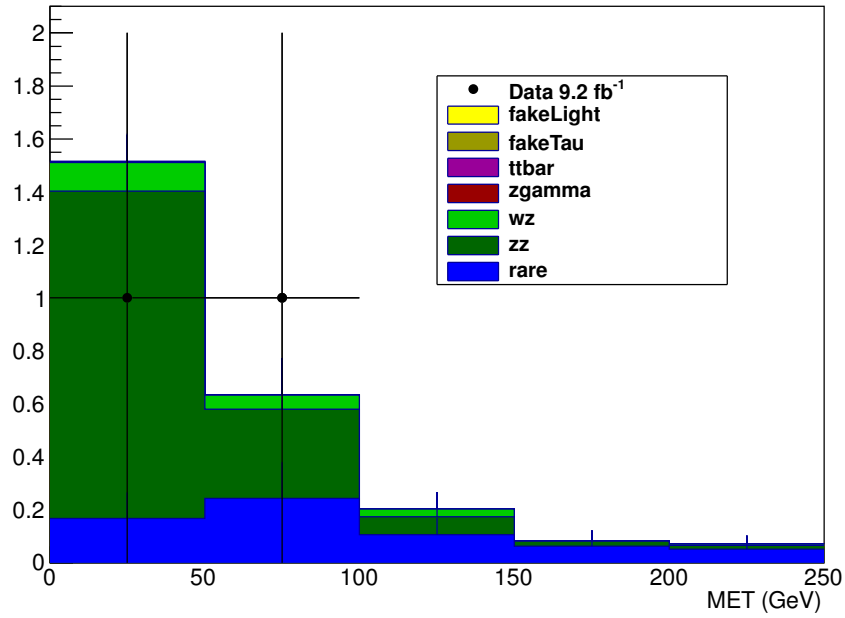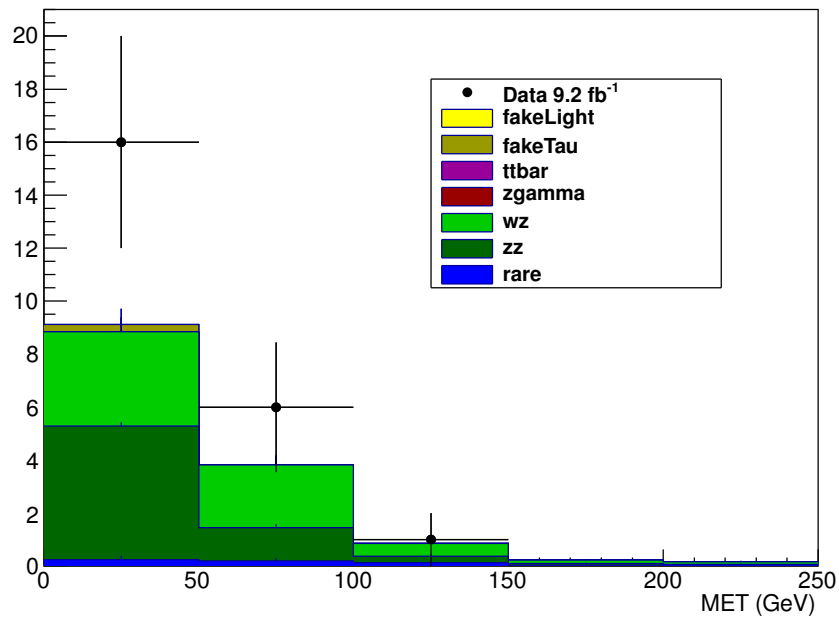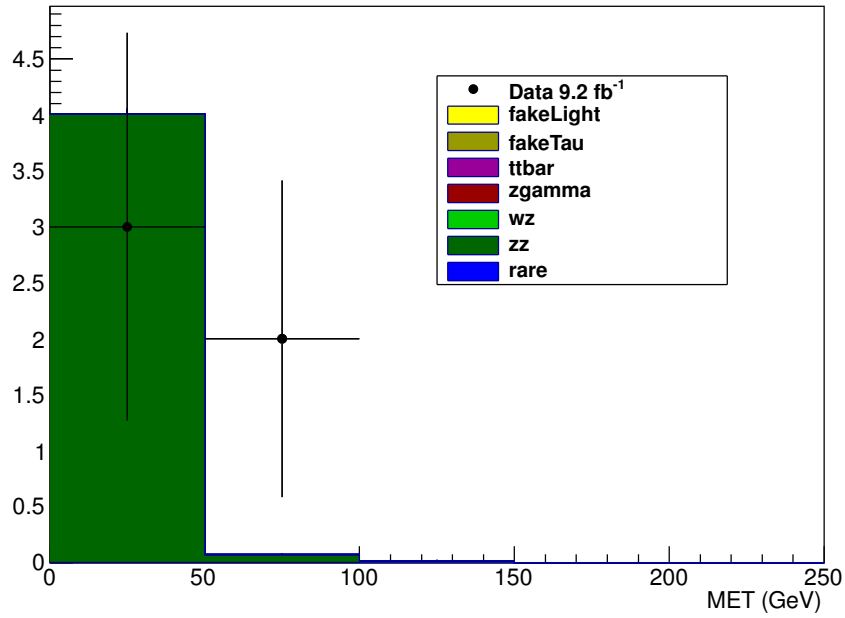

Figure 7: Observed yields and predicted backgrounds for four lepton events with no OSSF pairs and one tau.

Figure 8: Observed yields and predicted backgrounds for four lepton events with one OSSF pair offZ and zero taus.
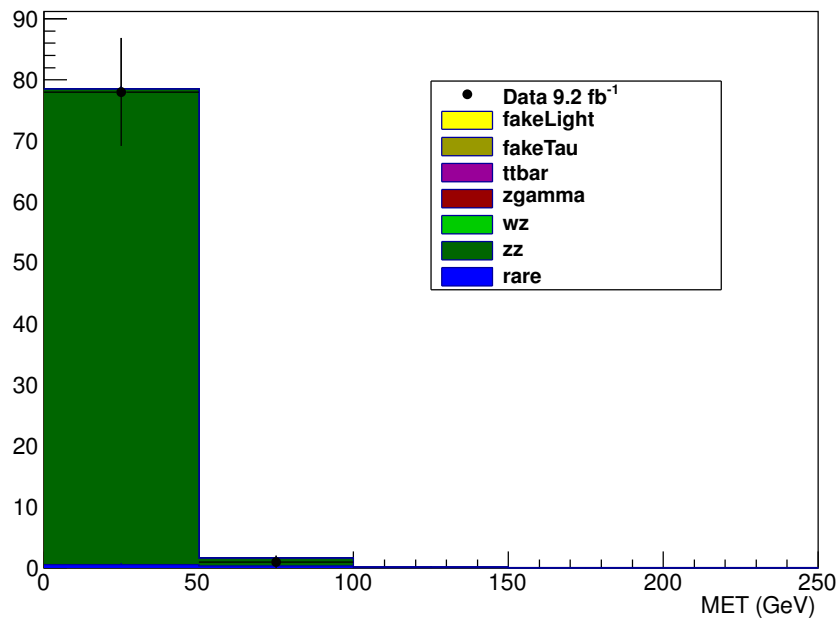

Figure 9: Observed yields and predicted backgrounds for four lepton events with one OSSF pair off Z and one tau.

Figure 10: Observed yields and predicted backgrounds for four lepton events with one OSSF pair on Z and zero taus.

Figure 11: Observed yields and predicted backgrounds for four lepton events with one OSSF pair on Z and one tau.

Figure 12: Observed yields and predicted backgrounds for four lepton events with two OSSF pairs offZ and zero taus.

Figure 13: Observed yields and predicted backgrounds for four lepton events with two OSSF pairs onZ and zero taus.
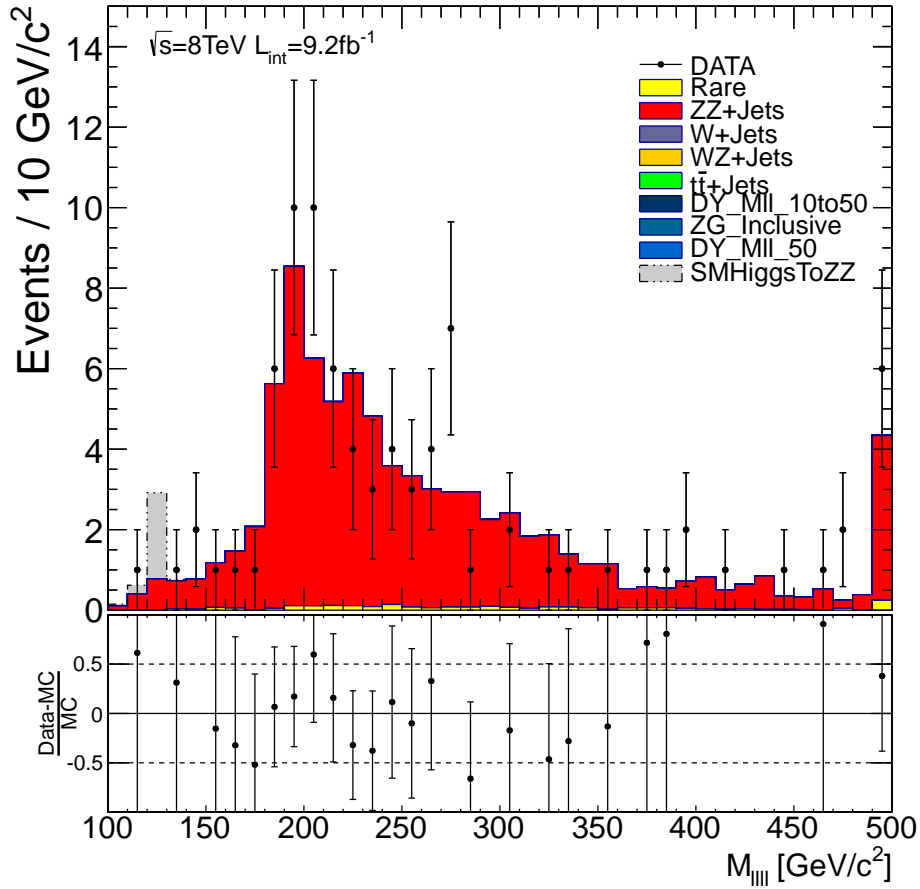
Figure 14: Invariant mass of all four leptons in the events with four leptons, two OSSF pairs, and zero leptons. For comparison, we show the Higgs to ZZ to 4L expected signal.

8   Statistical Procedure

To build a statistical model for this analysis we consider following sources of systematics shared (100% correlated between channels):

- uncertainties in luminosity, jet energy scale, trigger efficiency
- uncertainty of backgrounds: WZ, ZZ, $Z\gamma$, $t\bar{t}$, rare processes
- uncertainty of electron reconstruction, identification, selection efficiencies
- uncertainty of muon reconstruction, identification, selection efficiencies
- uncertainty of tau reconstruction, identification, selection efficiencies

Every channel also has two nuisances uncorrelated with other channels. These uncertainties account for statistical fluctuations affecting background estimations, and signal efficiency calculation. As the total number of nuisances is proportional to number of channels used, and therefore necessary computing resources rise exponentially with number of combined channels, we have to keep number of channels actually used for the analysis limited. For the given point in the model parameter space we select a predefined number (currently 10) of the most sensitive channels. The sensitivity of the channel is defined as an expected limit on the total model cross section obtained by using this channel only. This analysis is a typical multi-channel counting experiment. Higgs group combination tool, LandS [6], is technically used to obtain

Table 7: Four lepton backgrounds and observed yields. Backgrounds are given with statistical and systematic uncertainties, in that order.

E_T^{miss} (GeV)	Observed	Total Bkg	$Z\gamma^*$	Rare SM	$t\bar{t}$ and Fake	WZ	ZZ
DY2onZTau0							
0–30	69	68.52 ± 1.04 ± 20.18	0.08 ± 0.04 ± 0.04	0.33 ± 0.02 ± 0.18	0.01 ± 0.01 ± 0.00	0.01 ± 0.01 ± 0.00	68.09 ± 1.04 ± 20.18
30–50	9	9.31 ± 0.32 ± 3.08	0.10 ± 0.06 ± 0.05	0.21 ± 0.03 ± 0.12	0.01 ± 0.00 ± 0.00	0.01 ± 0.01 ± 0.00	8.98 ± 0.31 ± 3.08
50–100	1	1.67 ± 0.14 ± 0.56	0.00 ± 0.00 ± 0.00	0.32 ± 0.04 ± 0.17	0.01 ± 0.01 ± 0.00	0.02 ± 0.01 ± 0.01	1.31 ± 0.13 ± 0.54
> 100	0	0.31 ± 0.03 ± 0.12	0.00 ± 0.00 ± 0.00	0.21 ± 0.03 ± 0.11	0.00 ± 0.00 ± 0.00	0.00 ± 0.00 ± 0.00	0.09 ± 0.01 ± 0.04
DY1onZTau0							
0–30	0	3.94 ± 0.32 ± 1.32	2.15 ± 0.26 ± 1.16	0.10 ± 0.03 ± 0.05	0.02 ± 0.01 ± 0.00	0.03 ± 0.01 ± 0.01	1.64 ± 0.19 ± 0.64
30–50	1	0.71 ± 0.10 ± 0.18	0.07 ± 0.04 ± 0.04	0.07 ± 0.02 ± 0.04	0.02 ± 0.01 ± 0.00	0.03 ± 0.01 ± 0.01	0.51 ± 0.09 ± 0.17
50–100	1	0.74 ± 0.09 ± 0.17	0.00 ± 0.00 ± 0.00	0.24 ± 0.04 ± 0.13	0.03 ± 0.01 ± 0.00	0.03 ± 0.01 ± 0.01	0.44 ± 0.08 ± 0.11
> 100	0	0.36 ± 0.04 ± 0.12	0.00 ± 0.00 ± 0.00	0.22 ± 0.04 ± 0.12	0.01 ± 0.01 ± 0.00	0.02 ± 0.01 ± 0.01	0.11 ± 0.02 ± 0.03
DY2offZTau0							
0–30	3	3.86 ± 0.26 ± 1.03	1.64 ± 0.23 ± 0.88	0.00 ± 0.00 ± 0.00	0.00 ± 0.00 ± 0.00	0.00 ± 0.00 ± 0.00	2.23 ± 0.12 ± 0.54
30–50	0	0.42 ± 0.07 ± 0.15	0.12 ± 0.06 ± 0.06	0.00 ± 0.00 ± 0.00	0.00 ± 0.00 ± 0.00	0.00 ± 0.00 ± 0.00	0.30 ± 0.03 ± 0.13
50–100	2	0.04 ± 0.01 ± 0.03	0.00 ± 0.00 ± 0.00	0.00 ± 0.00 ± 0.00	0.00 ± 0.00 ± 0.00	0.01 ± 0.00 ± 0.00	0.03 ± 0.00 ± 0.02
> 100	0	0.02 ± 0.01 ± 0.01	0.00 ± 0.00 ± 0.00	0.01 ± 0.01 ± 0.01	0.00 ± 0.00 ± 0.00	0.00 ± 0.00 ± 0.00	0.01 ± 0.01 ± 0.01
DY1offZTau0							
0–30	1	2.72 ± 0.28 ± 1.33	2.46 ± 0.27 ± 1.33	0.00 ± 0.00 ± 0.00	0.00 ± 0.00 ± 0.00	0.01 ± 0.01 ± 0.00	0.23 ± 0.08 ± 0.10
30–50	0	0.23 ± 0.07 ± 0.10	0.18 ± 0.07 ± 0.09	0.01 ± 0.00 ± 0.00	0.01 ± 0.00 ± 0.00	0.01 ± 0.00 ± 0.00	0.04 ± 0.01 ± 0.01
50–100	0	0.14 ± 0.04 ± 0.03	0.00 ± 0.00 ± 0.00	0.04 ± 0.02 ± 0.02	0.01 ± 0.01 ± 0.00	0.01 ± 0.01 ± 0.00	0.08 ± 0.03 ± 0.02
> 100	0	0.03 ± 0.01 ± 0.01	0.00 ± 0.00 ± 0.00	0.02 ± 0.01 ± 0.01	0.00 ± 0.00 ± 0.00	0.00 ± 0.00 ± 0.00	0.01 ± 0.01 ± 0.01
DY0offZTau0							
0–30	0	0.60 ± 0.14 ± 0.33	0.60 ± 0.14 ± 0.33	0.00 ± 0.00 ± 0.00	0.00 ± 0.00 ± 0.00	0.00 ± 0.00 ± 0.00	0.00 ± 0.00 ± 0.00
30–50	0	0.17 ± 0.07 ± 0.09	0.17 ± 0.07 ± 0.09	0.00 ± 0.00 ± 0.00	0.00 ± 0.00 ± 0.00	0.00 ± 0.00 ± 0.00	0.00 ± 0.00 ± 0.00
50–100	0	0.03 ± 0.02 ± 0.01	0.00 ± 0.00 ± 0.00	0.00 ± 0.00 ± 0.00	0.00 ± 0.00 ± 0.00	0.00 ± 0.00 ± 0.00	0.02 ± 0.02 ± 0.01
> 100	0	0.00 ± 0.00 ± 0.01	0.00 ± 0.00 ± 0.00	0.00 ± 0.00 ± 0.00	0.00 ± 0.00 ± 0.00	0.00 ± 0.00 ± 0.00	0.00 ± 0.00 ± 0.01
DY1onZTau1							
0–30	13	11.33 ± 0.51 ± 2.44	0.75 ± 0.34 ± 0.29	0.18 ± 0.04 ± 0.10	1.09 ± 0.24 ± 0.14	0.74 ± 0.05 ± 0.21	8.57 ± 0.29 ± 2.40
30–50	4	5.50 ± 0.20 ± 0.73	0.00 ± 0.00 ± 0.00	0.06 ± 0.01 ± 0.03	0.98 ± 0.05 ± 0.05	1.00 ± 0.06 ± 0.29	3.45 ± 0.18 ± 0.67
50–100	6	4.93 ± 0.17 ± 0.55	0.00 ± 0.00 ± 0.00	0.19 ± 0.05 ± 0.10	1.18 ± 0.06 ± 0.06	1.16 ± 0.06 ± 0.33	2.39 ± 0.14 ± 0.42
> 100	1	1.62 ± 0.09 ± 0.19	0.00 ± 0.00 ± 0.00	0.21 ± 0.04 ± 0.11	0.37 ± 0.03 ± 0.02	0.32 ± 0.03 ± 0.09	0.72 ± 0.07 ± 0.12
DY1offZTau1							
0–30	4	5.44 ± 1.39 ± 1.37	1.01 ± 0.18 ± 0.55	0.03 ± 0.02 ± 0.02	2.67 ± 1.37 ± 1.16	0.15 ± 0.02 ± 0.04	1.58 ± 0.13 ± 0.47
30–50	2	1.72 ± 0.36 ± 0.30	0.55 ± 0.28 ± 0.17	0.01 ± 0.01 ± 0.01	0.14 ± 0.02 ± 0.01	0.14 ± 0.02 ± 0.04	0.87 ± 0.22 ± 0.24
50–100	2	1.02 ± 0.15 ± 0.13	0.09 ± 0.11 ± 0.04	0.07 ± 0.03 ± 0.04	0.18 ± 0.02 ± 0.01	0.20 ± 0.02 ± 0.06	0.48 ± 0.09 ± 0.10
> 100	3	0.31 ± 0.06 ± 0.06	0.00 ± 0.00 ± 0.00	0.07 ± 0.03 ± 0.04	0.04 ± 0.01 ± 0.00	0.03 ± 0.01 ± 0.01	0.18 ± 0.05 ± 0.04
DY0offZTau1							
0–30	1	0.23 ± 0.07 ± 0.07	0.08 ± 0.05 ± 0.05	0.00 ± 0.00 ± 0.00	0.00 ± 0.00 ± 0.00	0.00 ± 0.00 ± 0.00	0.14 ± 0.06 ± 0.05
30–50	0	0.13 ± 0.05 ± 0.03	0.02 ± 0.02 ± 0.01	0.04 ± 0.04 ± 0.02	0.00 ± 0.00 ± 0.00	0.00 ± 0.00 ± 0.00	0.06 ± 0.03 ± 0.02
50–100	1	0.24 ± 0.09 ± 0.04	0.03 ± 0.07 ± 0.02	0.00 ± 0.00 ± 0.00	0.04 ± 0.01 ± 0.01	0.03 ± 0.01 ± 0.01	0.14 ± 0.06 ± 0.03
> 100	0	0.63 ± 0.32 ± 0.18	0.20 ± 0.18 ± 0.10	0.04 ± 0.03 ± 0.02	0.17 ± 0.17 ± 0.09	0.00 ± 0.00 ± 0.00	0.22 ± 0.20 ± 0.11

69 limits. We calculate "LHC style" CLs limit [7], which effectively means using frequentist CLs
70 with one-sided profiled likelihood test statistics.

8.1 Limits on SMS from the search with three leptons and from same-sign di-lepton searches

73 Figure 15 displays, for $x_{\tilde{\ell}} = 0.5$, the results of the three-lepton search using $E_{\mathrm{T}}^{\mathrm{miss}}$, M_{T} and $M_{\ell\ell}$.
74 The figure depicts 95% CL upper limit on the cross section times branching fraction in the $m_{\tilde{\chi}_1^0}$
75 versus $m_{\tilde{\chi}_2^0}$ ($= m_{\tilde{\chi}_1^\pm}$) plane in the flavor-democratic scenario. The contour bounds the excluded
76 region in the plane assuming the NLO cross section calculation and a 50% branching fraction,
77 as appropriate for the visible decay products in this scenario. Figure 16 shows the results for
78 two values $x_{\tilde{\ell}}$ (0.05 and 0.95) obtained after combination of three-lepton and the SS di-lepton
79 searches [8].

80 Figure 17 presents the corresponding limits for the τ-enriched scenario and Figure 18 for the
81 τ-dominated scenario. As the SS di-lepton search does not have sensitivity for $x_{\tilde{\ell}} = 0.50$, there
82 is no limit curve for this search for Figures 15, 17b and 18. In the other limit curves in both
83 Figures 16 and 17, the increase in the combined mass limit from incorporation of the SS di-lepton
84 lepton search ranges up to approximately 20 GeV.

8.2 Limits on SMS with on-shell W and Z from WZ + $E_{\mathrm{T}}^{\mathrm{miss}}$ and three-lepton analyses

87 For limits on the SMS with on-shell W and Z bosons, we show the results of the WZ + $E_{\mathrm{T}}^{\mathrm{miss}}$
88 analysis [9], the three-lepton analysis as well as the combined result.

89 In the combination, the common signal-related systematic uncertainties for luminosity, jet en-
90 ergy scale, lepton identification, trigger efficiency, and misidentification of light-flavor jets as
91 b jets are considered to be 100% correlated. For backgrounds, the only common systematic un-
92 certainty is that for the WZ simulation, which is treated as 100% correlated. No events in the
93 data pass both signal selections. For the backgrounds, the overlap in the control sample is less
94 than 1%. Thus the two selections are treated as independent.

95 Figure 19 displays the observed limits for the two individual analyses and the combination.

9 Conclusion

97 This analysis note presents a summary for searches for supersymmetric charginos and neu-
98 tralinos in three and four leptons final states which were developed and presented in several
99 analysis notes. The searches featured here explore the final states with exactly three or exactly
100 four leptons using transverse mass, missing transverse energy and lepton-pair invariant mass.
101 No excesses above the standard model expectations are observed. The results are used to ex-
102 clude a range of chargino and neutralino masses for the models considered in the dedicated
103 analyses where these particles have large branching fractions to leptons and vector bosons.
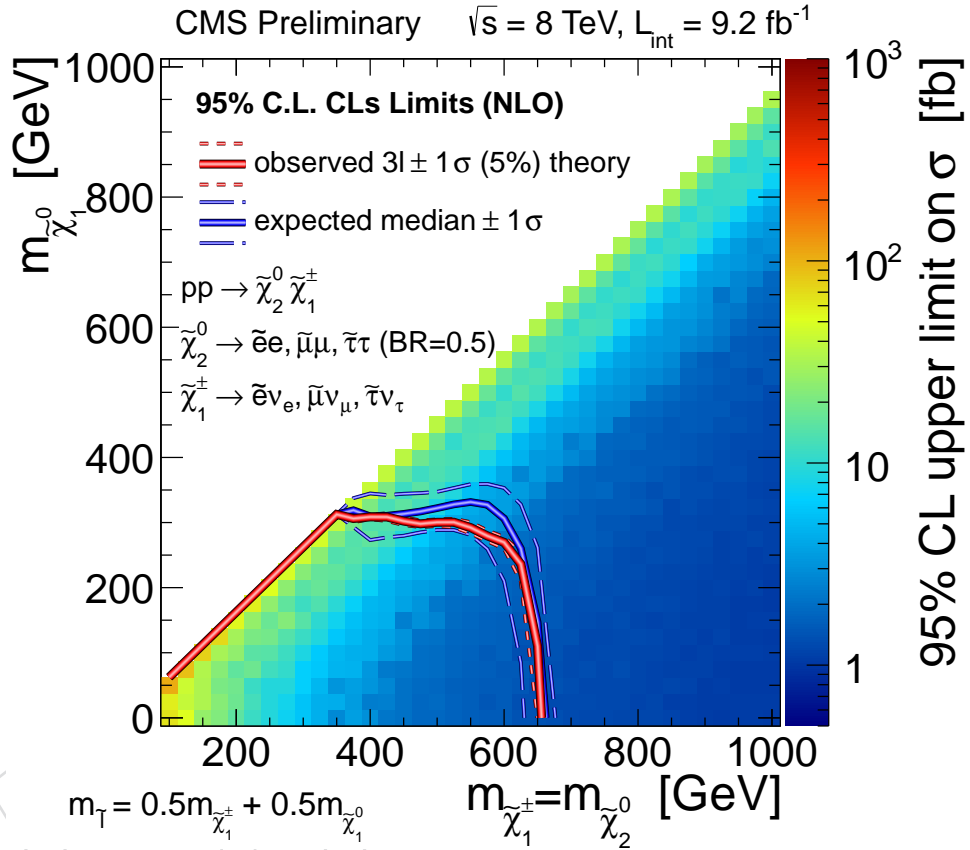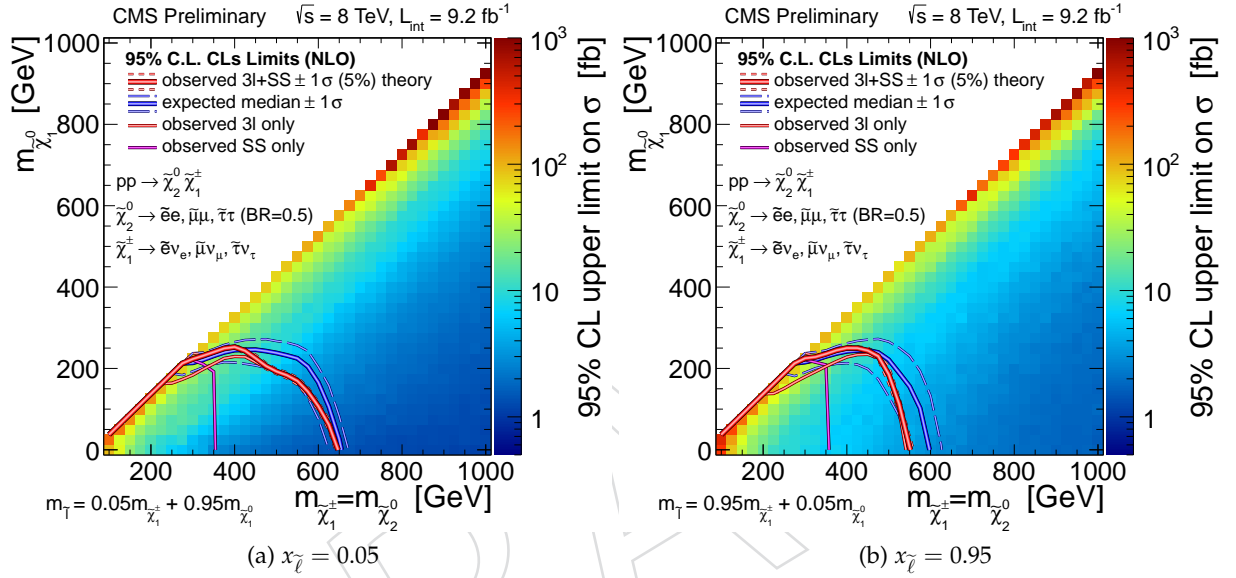
Figure 15: The shading in the $m_{\widetilde{\chi}_1^0}$ versus $m_{\widetilde{\chi}_2^0}$ ($= m_{\widetilde{\chi}_1^\pm}$) plane indicates the 95% CL upper limit on the chargino-neutralino production NLO cross section times branching fraction in the flavor-democratic scenario, for the three-lepton search. The contours bound the mass regions excluded at 95% CL for a branching fraction of 50%, as appropriate for the visible decay products in this scenario. The contours based on the observations are shown; in addition, the expected bound is shown.

(a) $x_{\tilde{\ell}} = 0.05$ (b) $x_{\tilde{\ell}} = 0.95$

Figure 16: The shading in the $m_{\tilde{\chi}_1^0}$ versus $m_{\tilde{\chi}_2^0}$ $(= m_{\tilde{\chi}_1^\pm})$ plane indicates the 95% CL upper limit on the chargino-neutralino production NLO cross section times branching fraction in the flavor-democratic scenario, for the combined analysis of the three-lepton search and the same-sign di-lepton search. The contours bound the mass regions excluded at 95% CL for a branching fraction of 50%, as appropriate for the visible decay products in this scenario. The contours based on the observations are shown for the combination; in addition, the expected combined bound is shown. Red contours demonstrate separate mass exclusions for the three-lepton search and the same-sign di-lepton search alone.

(a) $x_{\tilde{\ell}} = 0.05$

(b) $x_{\tilde{\ell}} = 0.5$

(c) $x_{\tilde{\ell}} = 0.95$
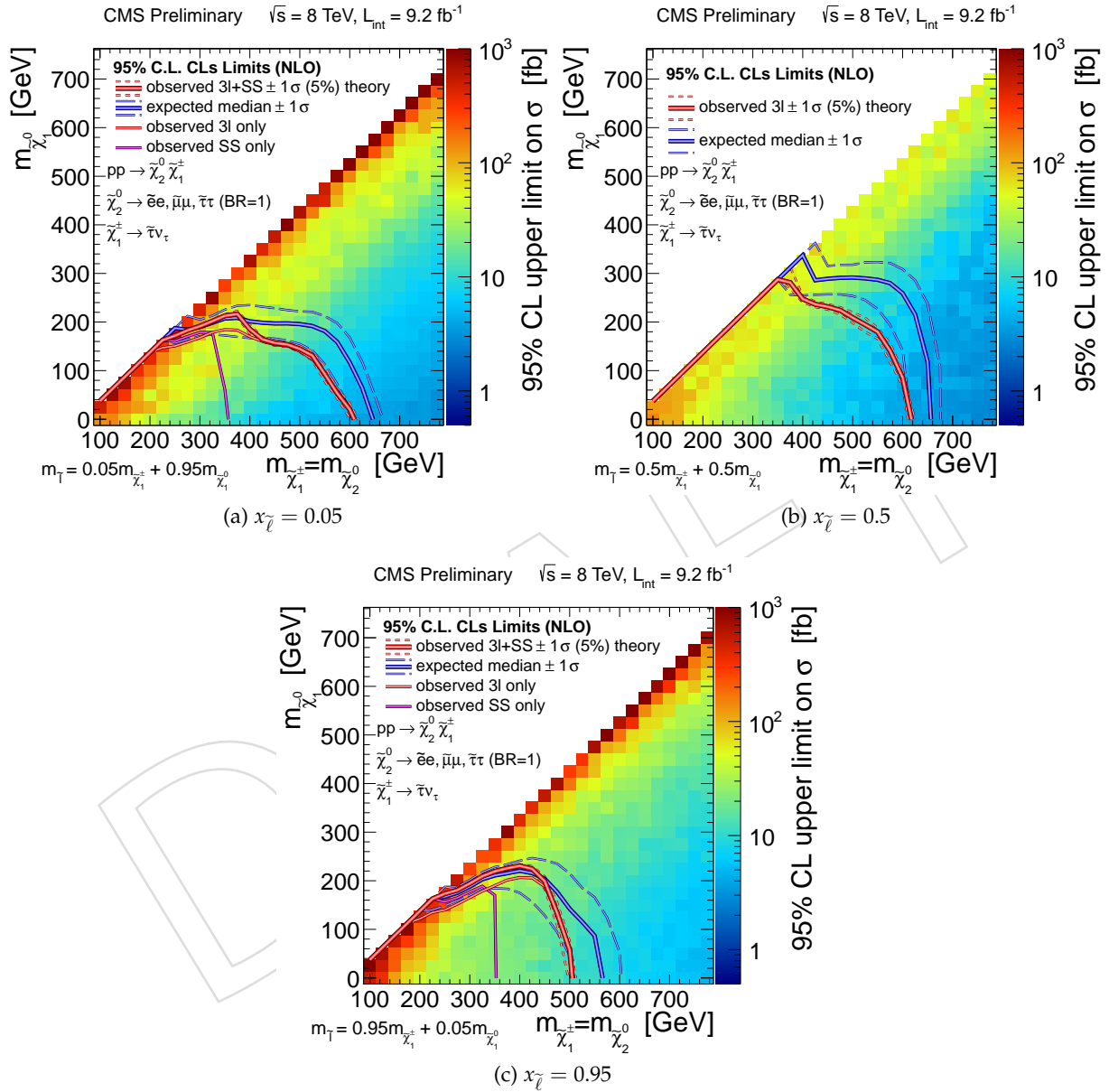
Figure 17: The exclusion contours for τ-enriched scenario corresponding to results in Figure 15: (a) and (c) combination of 3-lepton searches with SS d-lepton analysis, (b) 3 lepton searches.
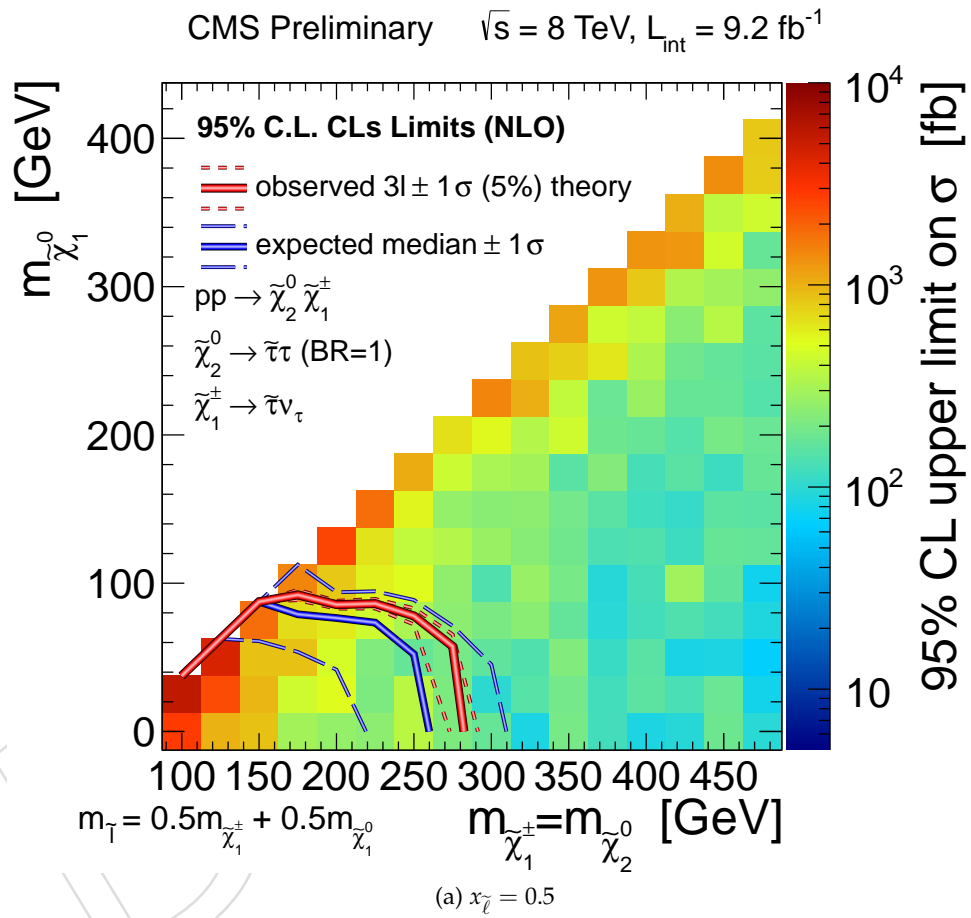
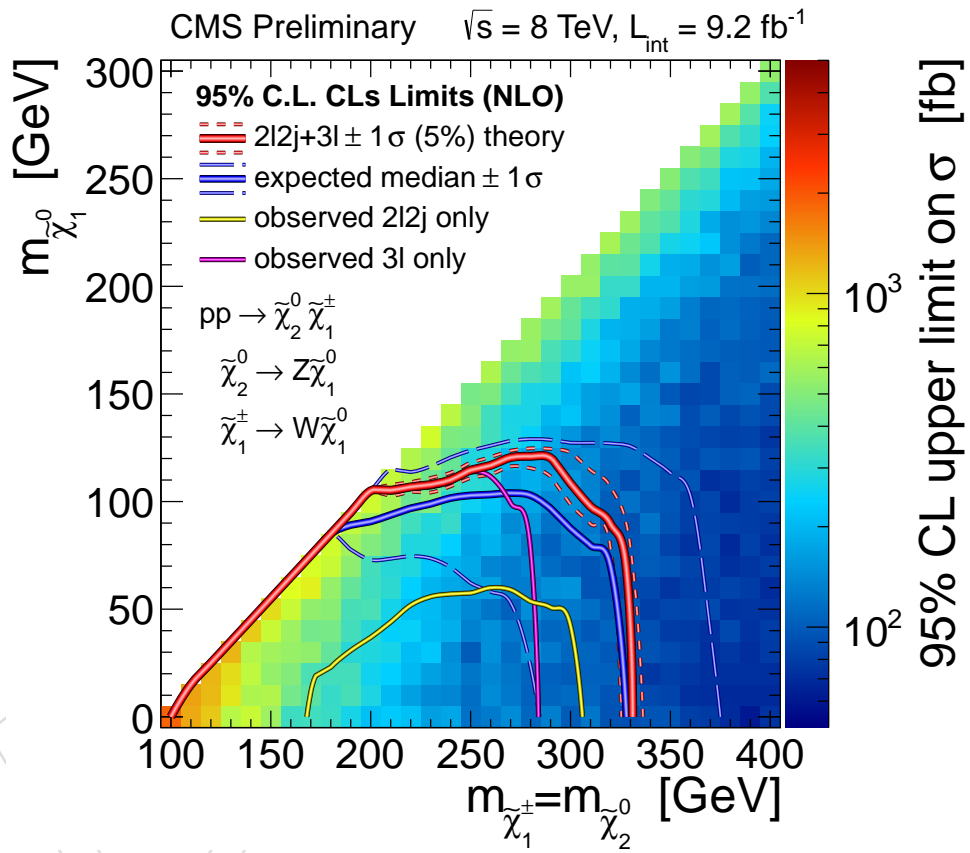Figure 18: The exclusion contours for τ-dominated scenario corresponding to results in Figure 15.

Figure 19: Interpretation of the WZ + E_T^{miss} and three-lepton results in the context of the WZ SMS. The WZ+ E_T^{miss} observed, three-lepton observed, combined observed, and combined expected contours are indicated.

A   Graphical Comparison of the Background Estimations

The efforts described in works [2–4] are summarised for a review in the plots presented in this section. If not stated explicitly, the black color in the plots corresponds to a Ref. [2], the red color to a Ref. [3], and the blue color to a Ref. [4]. While for the tri-lepton processes without a tau three results are compared, for channels with a tau present contribution were made by two out of three works which are presented in the plots.

References

[1] CMS Collaboration, "Search for direct EWK production of SUSY particles in multilepton modes with 8TeV data", CMS Physics Analysis Summary CMS-PAS-SUS-12-022, (2012).

[2] M. Chen et al., "Search for Direct Electroweak Production of Charginos and Neutralinos with the Tri-lepton Plus Missing Energy Final State", CMS Analysis Note AN/2012-248, (2012).

[3] W. de Boer et al., "Search for SUSY using signatures with at least three leptons and missing transverse energy and/or high jet activity at $\sqrt{s}$=8 TeV", CMS Analysis Note AN/2012-255, (2012).

[4] S. Arora et al., "A Search for Direct Chargino Neutralino production with three or more leptons using 9.5 fb^{-1} of $\sqrt{s}$=8 TeV CMS data", CMS Analysis Note AN/2012-256, (2012).

[5] S. Arora et al., "Background and Efficiency Determination Methods for Multilepton Analyses", CMS Analysis Note AN/2012-257, (2012).

[6] M. Chen., "LandS: A statistical tool for calculating limits and significance". https://mschen.web.cern.ch/mschen/LandS/index.html, April, 2011.

[7] "Procedure for the LHC Higgs boson search combination in summer 2011", Technical Report ATL-PHYS-PUB-2011-011, CMS NOTE-2011/005, CERN, Geneva, (Aug, 2011).

[8] M. Dünser, S. Folgueras, F. Moortgat et al., "Search for Direct Production of Charginos and Neutralinos in the Same-Sign Di-Lepton Channel Using 8TeV pp Collisions", CMS Analysis Note AN/2012-330, (2012).

[9] D. Barge, C. Campagnari, D. Kovalskyi et al., "Search for beyond-the-standard model physics in events with a Z boson, jets, and missing transverse energy", CMS Analysis Note AN/2012-254, (2012).
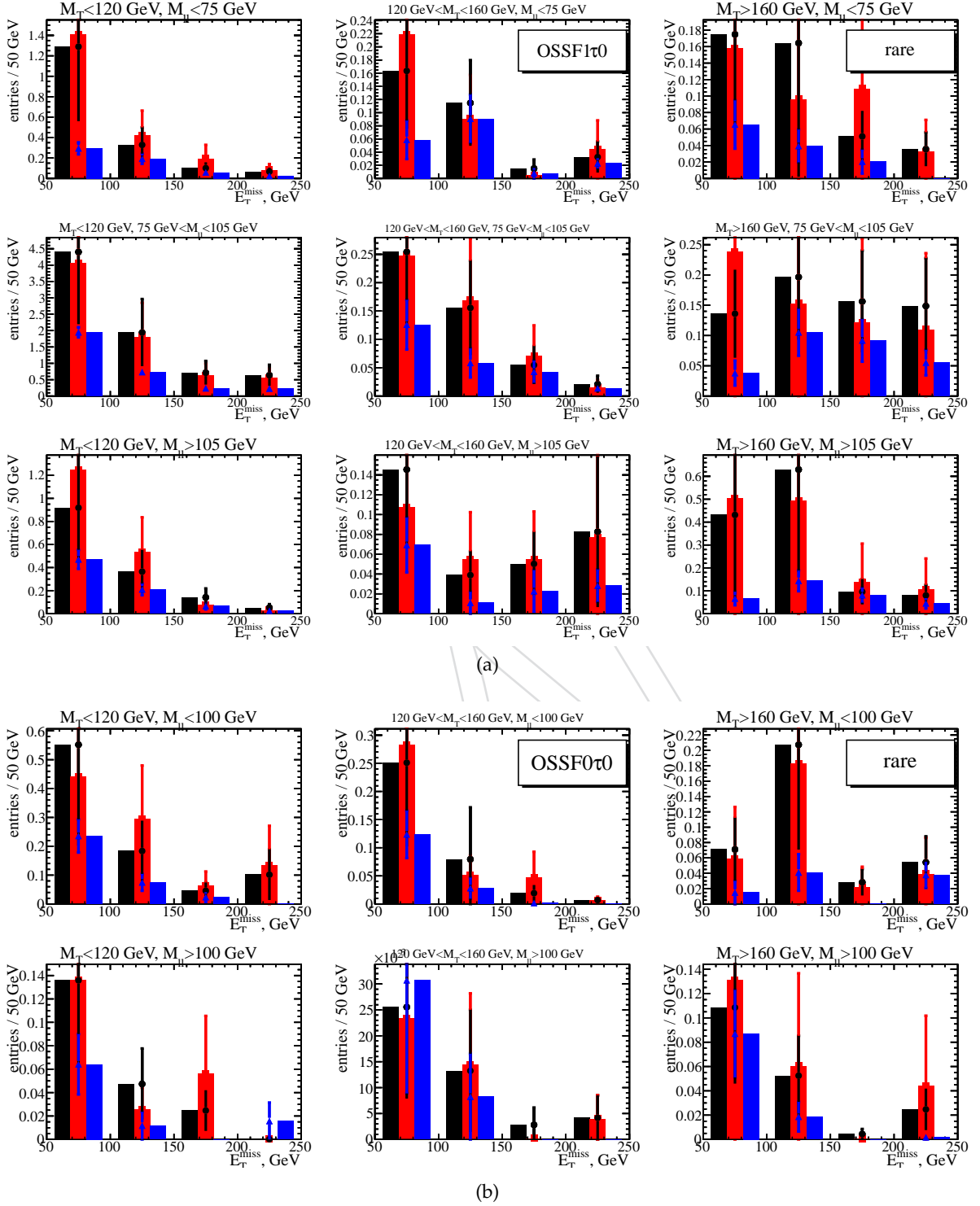
(a)

(b)

Figure 20: Comparison of the Rare SM contribution. Blue histograms from Ref. [4] do not fully take into account all the processes therefore their contribution is excluded from the final combination.
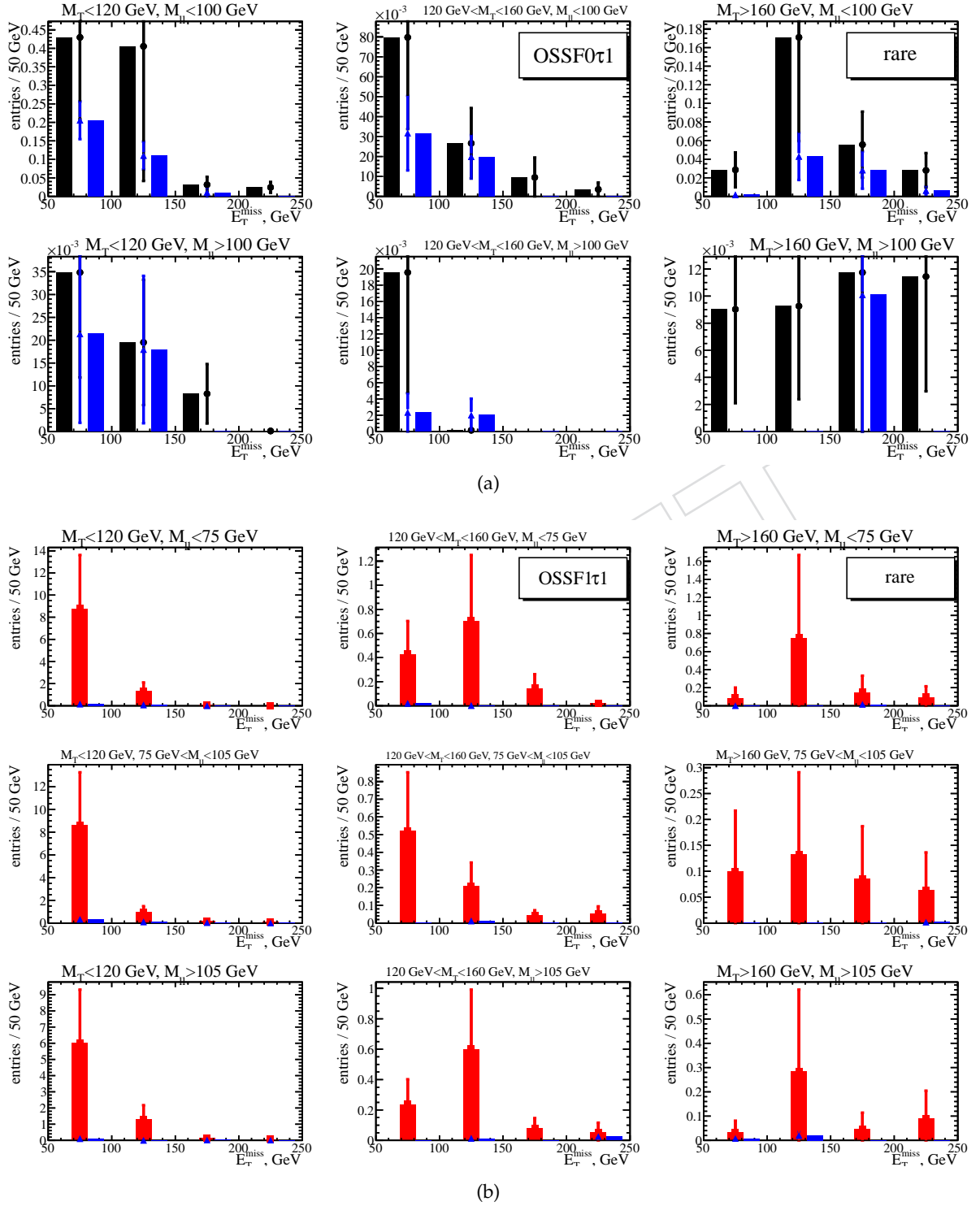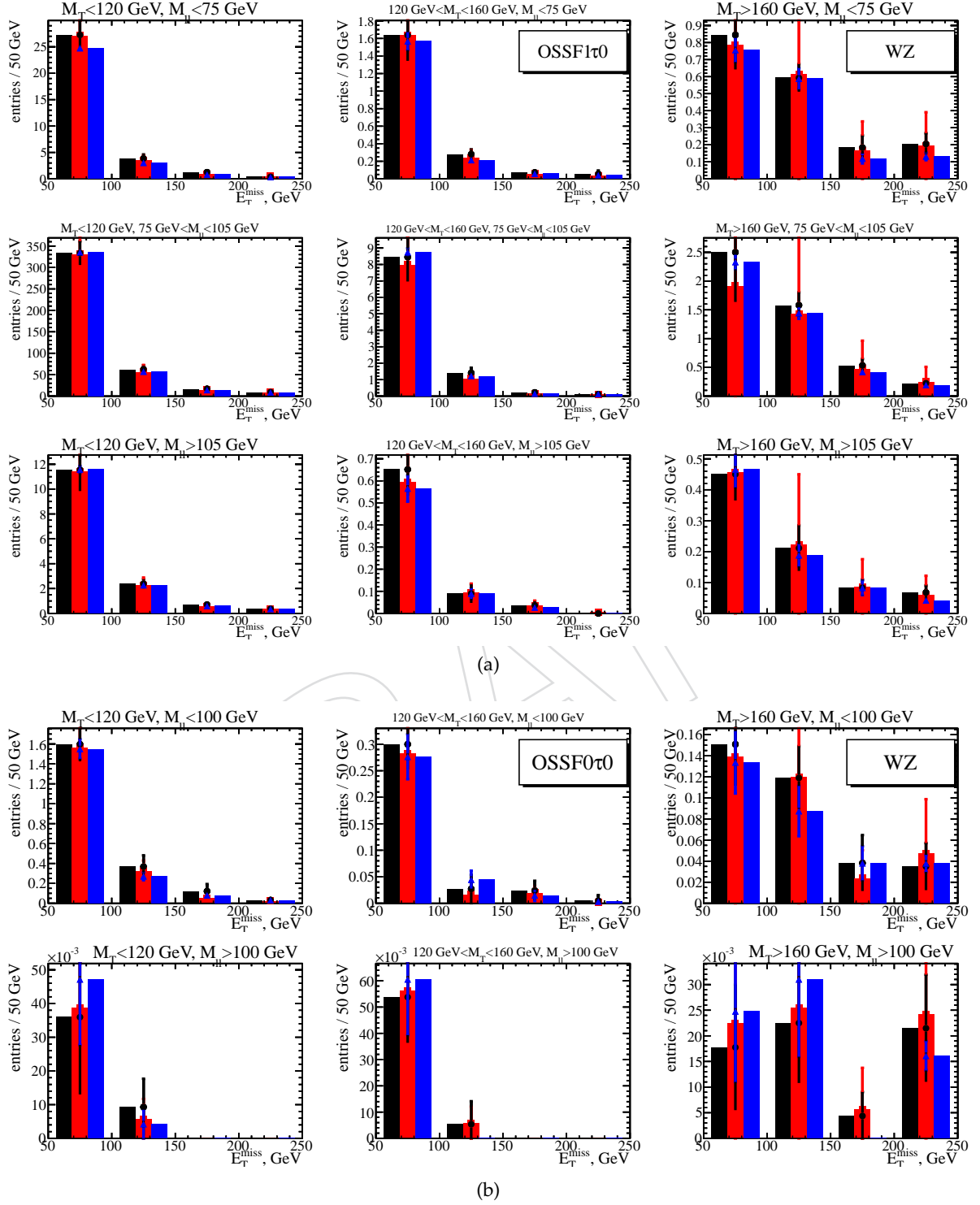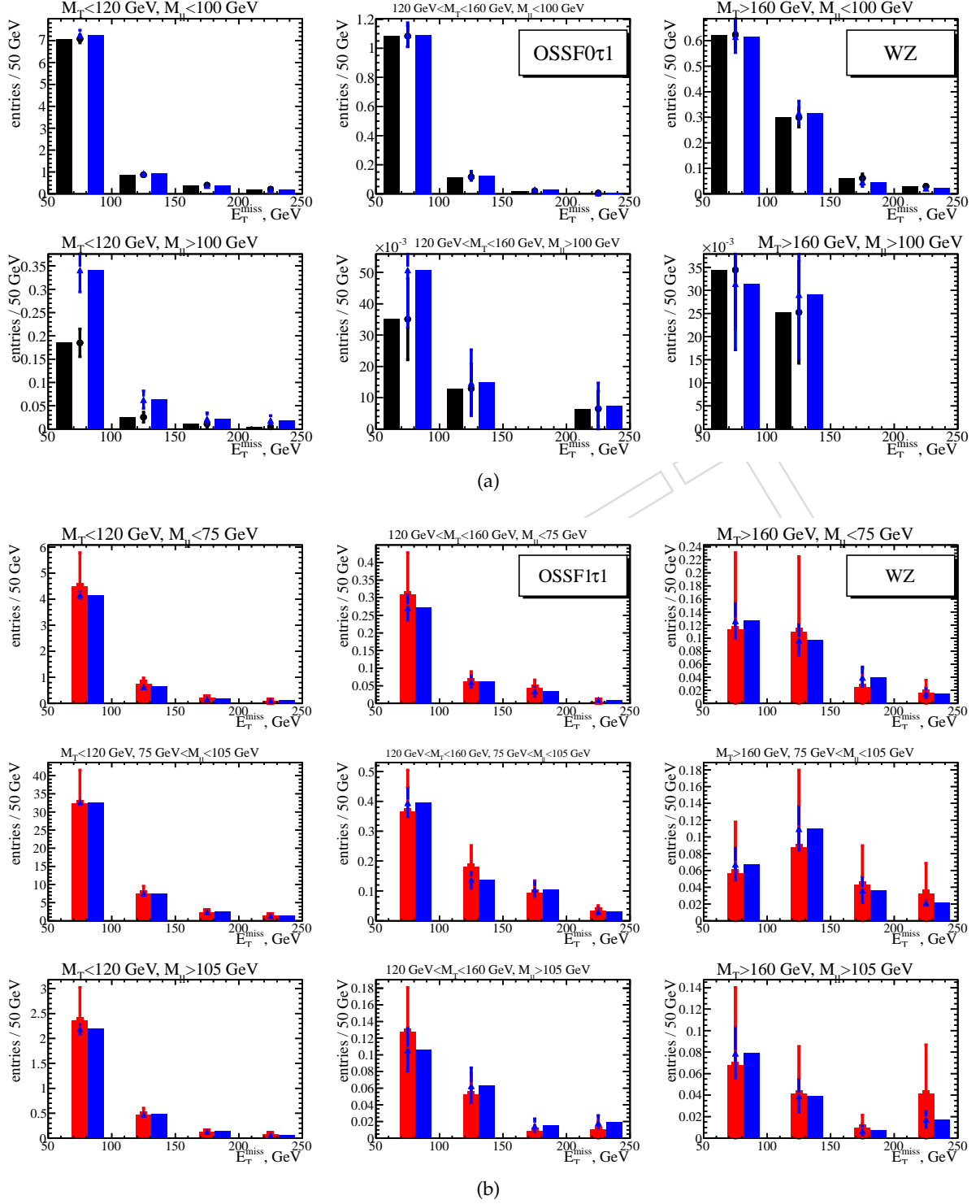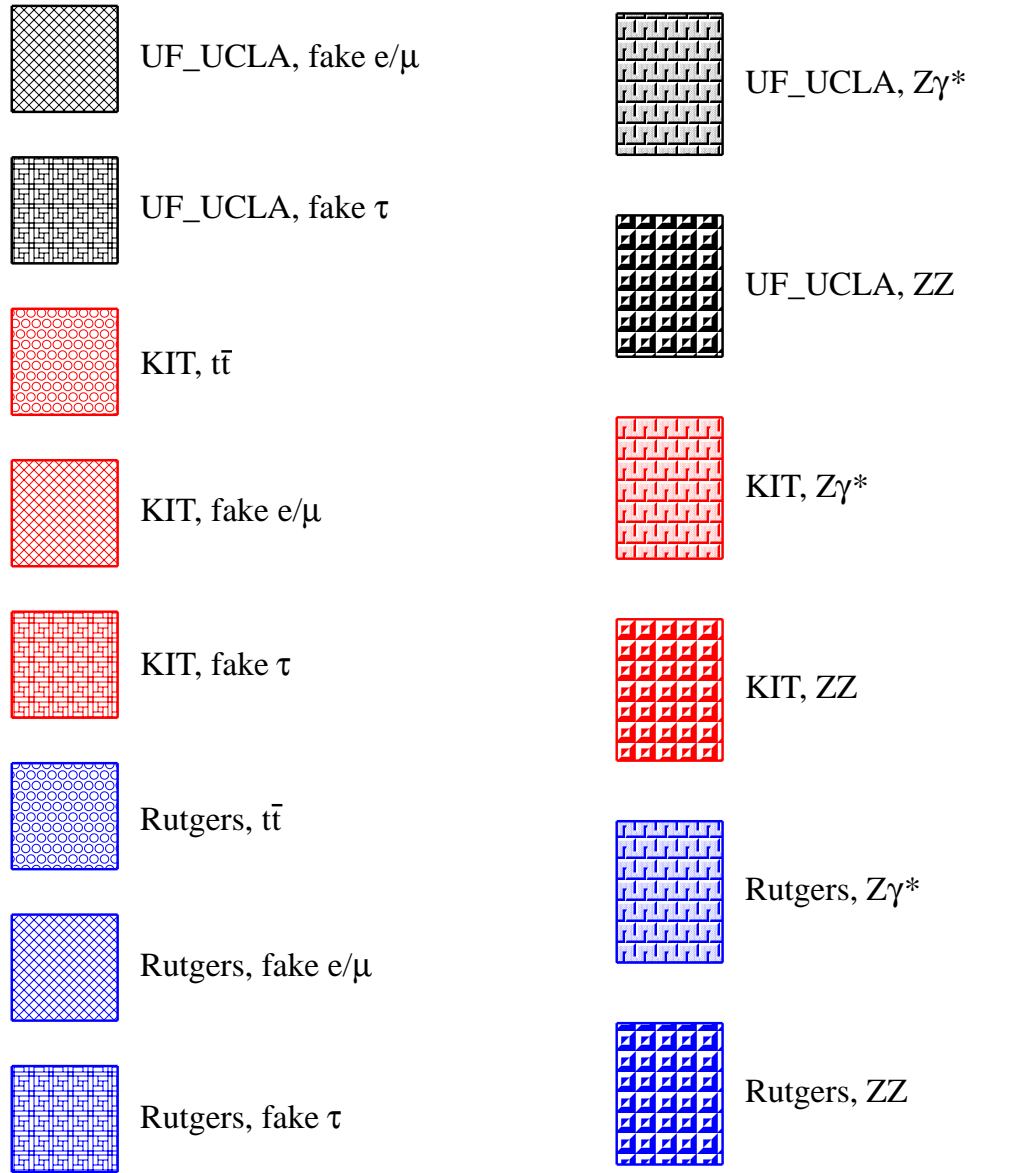
(a)

(b)

Figure 21: Comparison of the Rare SM contribution. Blue histograms from Ref. [4] do not fully take into account all the processes therefore their contribution is excluded from the final combination.

(a)

(b)

Figure 22: Comparison of the *WZ* backgrounds.

(a)

(b)
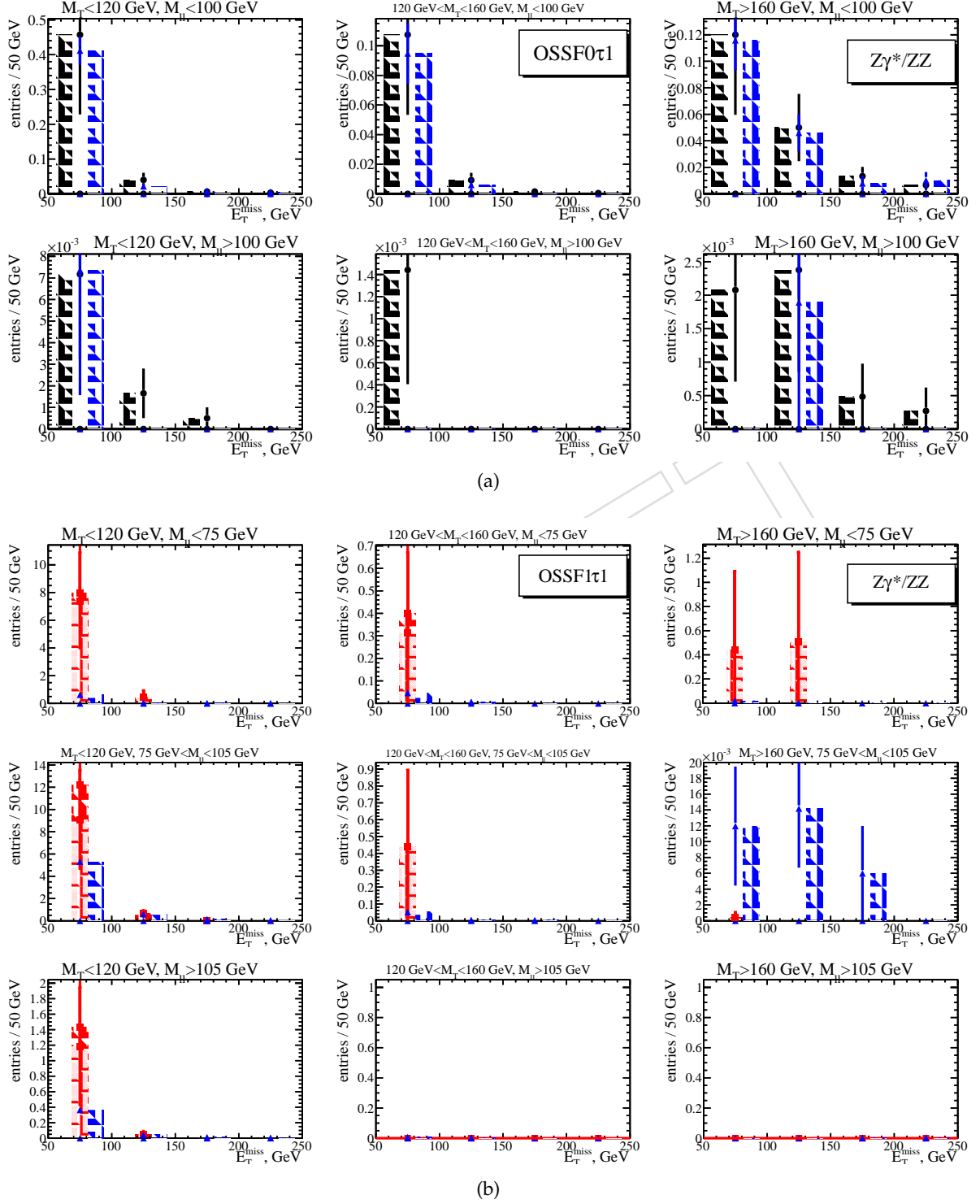
Figure 23: Comparison of the *WZ* backgrounds.

(a) Non-prompt leptons legend.   (b) ZZ and $Z\gamma^*$ legend.

Figure 24: Legends for the following plots.

(a)

(b)
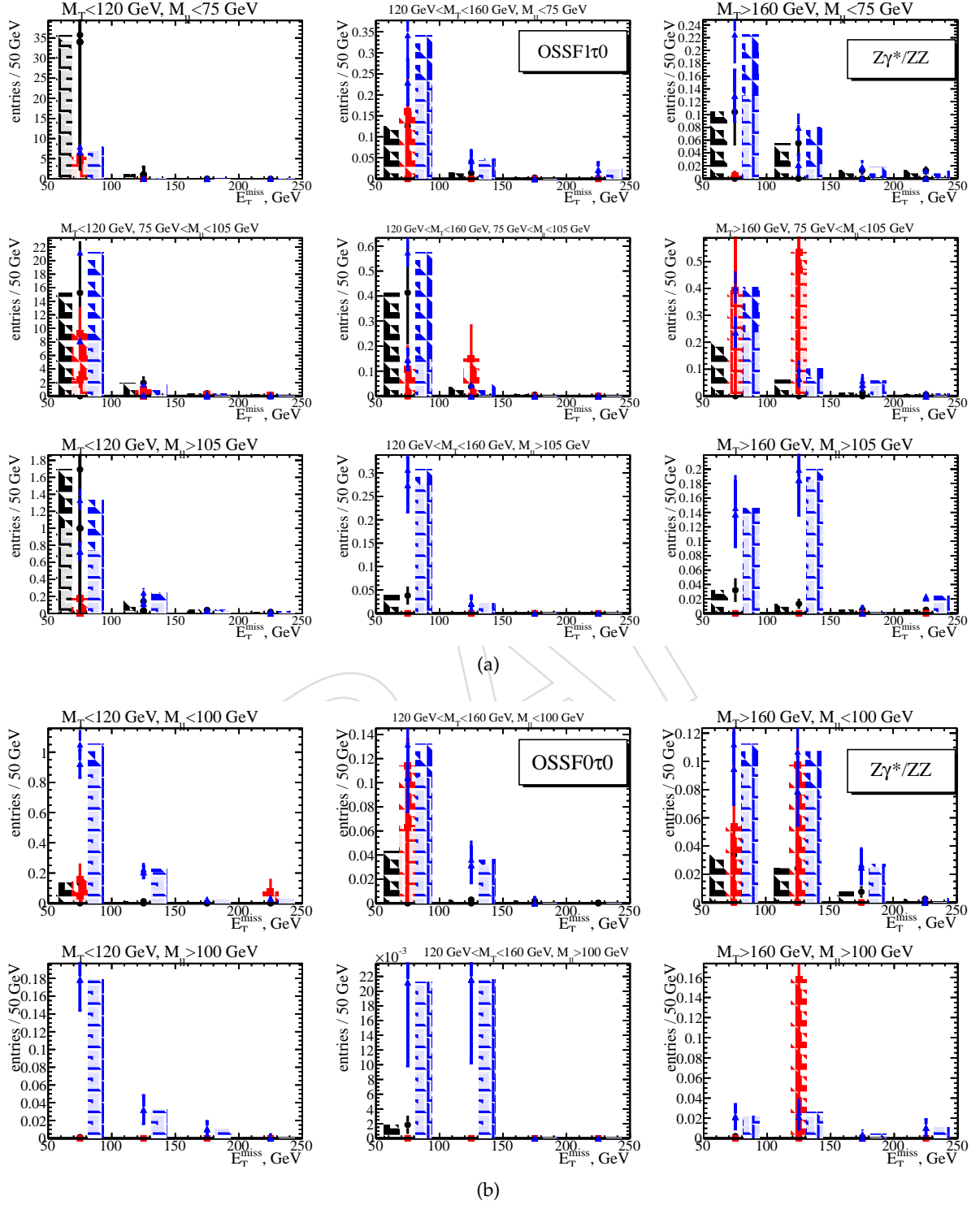
Figure 25: Comparison of the ZZ and $Z\gamma^*$ contribution.

(a)

(b)

Figure 26: Comparison of the ZZ and $Z\gamma^*$ contribution.
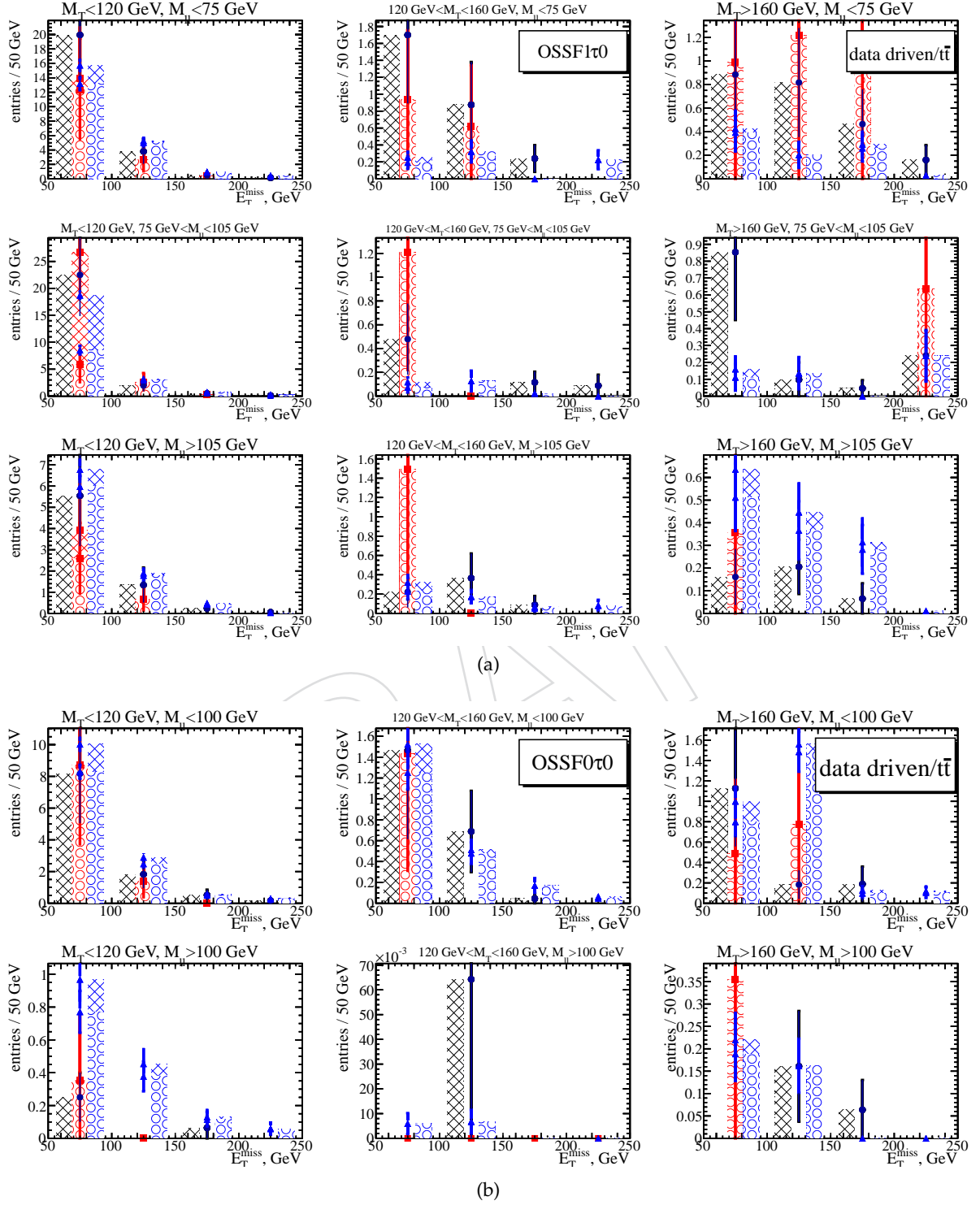
(a)

(b)

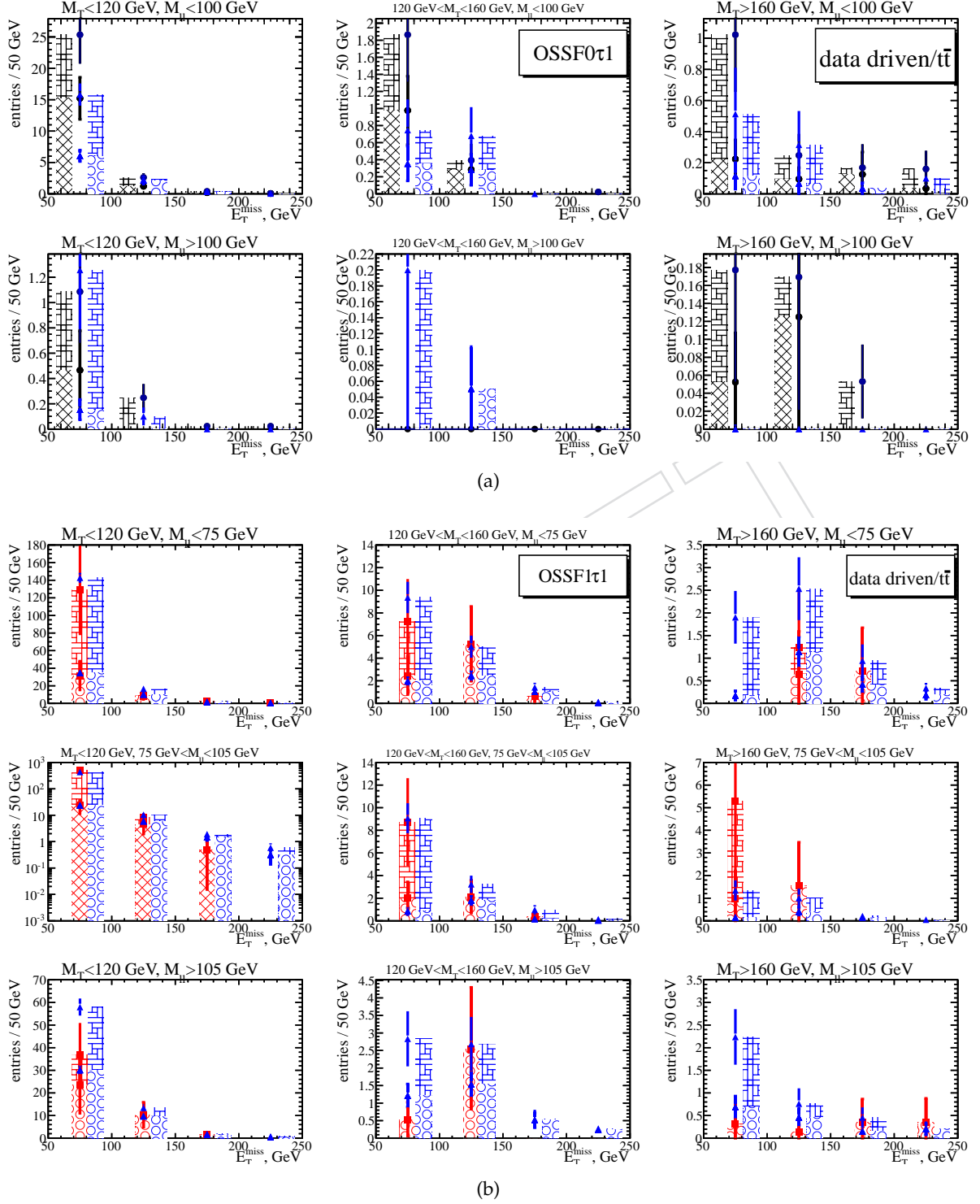Figure 27: Comparison of the non-prompt leptons contribution.

(a)

(b)

Figure 28: Comparison of the non-prompt leptons contribution.